GEOLOGIC MAP OF THE

BLACK HILL 7.5-MINUTE QUADRANGLE,

SOCORRO COUNTY, NEW MEXICO

By
Andrew P. Jochems and Daniel J. Koning

June 2019

New Mexico Bureau of Geology and Mineral Resources
Open-file Digital Geologic Map OF-GM 274

Scale 1:24,000

This work was supported by the U.S. Geological Survey, National Cooperative Geologic Mapping Program (STATEMAP) under USGS Cooperative Agreement G18AC00201 and the New Mexico Bureau of Geology and Mineral Resources.

New Mexico Bureau of Geology and Mineral Resources, New Mexico Institute of Mining and Technology, 801 Leroy Place, Socorro, New Mexico, 87801-4796

CONTENTS

Note on Private-Land Access in the Map Area

The Black Hill 7.5-minute quadrangle contains significant acreages of public land (Bureau of Land Management or State of New Mexico) but parcels of private land do exist, primarily along Nogal Canyon and west of New Mexico Highway 1. We ask that all users of this map obtain permission from local owners before entering their lands.

EXECUTIVE SUMMARY

The Black Hill 7.5-minute quadrangle is located in the southern part of the San Marcial Basin, an east-tilted half graben in the southern Rio Grande rift. The map area includes uplands cored by Paleogene volcanic and Paleozoic carbonate rocks in the southwest, a large paleofan extending from the foothills of the San Mateo Mountains in the central and southern parts of the quadrangle, and a number of tributaries to the Rio Grande. Among the latter, from north to south, are: Sheep Canyon, Lumbre Canyon, Crawford Hollow, Silver Canyon, Nogal Canyon, and Chaunte Canyon. Nogal Canyon forms an impressive gorge crossed by Interstate 25 and features local relief of up to 185 m where it runs adjacent to bedrock hills in the southwestern quadrangle.

The oldest rocks exposed in the quadrangle are Paleozoic limestones thought to be Pennsylvanian in age (Pu); these underlie two hills south of Nogal Canyon and several small exposures in the northwestern part of the map area. Eocene to Oligocene volcanic rocks underlie prominent hills and ridges along New Mexico Highway 1 and south of Crawford Hollow to the southern quadrangle boundary. These include a trachyandesite (Tta), Tuff of Rocque Ramos Canyon (Trr), La Jencia Tuff (Tlj), and Vicks Peak Tuff (Tvp) as well as a minor volcaniclastic unit (Tvs). All tuffs are outflow facies although the Vicks Peak is within 6-8 km of the southeastern margin of its source caldera.

Early Pleistocene through Miocene basin-fill deposits dominate the geology of the quadrangle. Fine-grained basin fill inferred to be Miocene in age is found along Nogal Canyon in its deeper reaches near the western quadrangle boundary. Plio-Pleistocene gravel, sand, silt, and clay belonging to the Palomas Formation lie above this older basin fill, attaining a minimum thickness of 180 m. The Palomas Formation transitions from mostly coarse-grained piedmont facies in the west to sandy axial-fluvial facies in the east. Younger deposits (middle Pleistocene to Holocene) include alluvial fans, well-defined suites of terraces in the major drainages, and valley-floor alluvium. A series of erosional surfaces have formed on the Palomas Formation north of Crawford Hollow. Shallow aquifers of moderate- to high-quality groundwater are likely to be found in late Quaternary valley fill and deeper groundwater sources may exist in the Palomas Formation, particularly the sandy, uncemented axial-fluvial facies.

The Palomas Formation piedmont facies units exposed in the quadrangle were deposited on hanging-wall distributary fan systems emanating from the foothills of the southeastern San Mateo Mountains. Of note is the large Nogal Canyon paleofan with a northern margin near Crawford Hollow and a major control on the modern, fanning topography in the southern 2/3 of the quadrangle. Modern Nogal Canyon apparently runs south of the main axis of this paleofan. The Palomas Formation axial-fluvial units were deposited in braided channels or floodplain environments of the ancestral Rio Grande. In total, six conformable member-rank units were mapped for the Palomas Formation.

The lower piedmont facies (Tppl) consists of 35-45 m of gravel/conglomerate containing pebbles through boulders deposited by debris flows in proximal alluvial fan environments. This unit is best exposed in low-lying ridges around the southwestern quadrangle. The undivided lower to middle piedmont facies (QTppml) was mapped in parts of Nogal Canyon not accessed due to land permission restrictions, but probably consists of <60 m of silty or sandy sediment and gravel that may coarsen to the west. The middle piedmont facies (QTppm) is dominated by extra-channel silt and mud with subordinate fluvial or debris-flow sand and gravels and minor calcareous *ciénega* deposits found at distal fan positions in the eastern quadrangle. The middle piedmont facies have a maximum thickness of at least 60 m. The upper piedmont facies (Qppu) includes interbedded gravel bodies, pebbly silt-sand, silt, and mud with a maximum thickness of 85 m. In Nogal Canyon, near and upstream of Interstate 25, this unit consists almost entirely of stacked gravel deposits deposited by debris flows. It is distinguished from the middle piedmont facies by redder colors, a greater proportion of matrix clay, and sheet-like geometries among its gravel beds.

The axial-fluvial facies of the Palomas Formation (QTpa)

consists of fine- to coarse-grained, quartzose sand with subordinate gypsiferous mud and pebble gravel beds, the latter containing exotic clast lithologies such as chert, granite, and quartzite. Its total thickness is unknown but projections of contacts from cross-section A-A' and well data indicate a minimum thickness of 70-75 m in the Silver Canyon area. Vertebrate fossils recovered from channel-margin deposits of unit QTpa indicate a Blancan age for the unit, with its top younger than ~2.7 Ma. A thin, fine-grained subunit (QTpaf) found in Crawford Hollow consisting of massive mud represents floodplain deposition and interfingers with the middle piedmont facies. In most of the quadrangle, the upper piedmont facies as prograded over the axial-fluvial facies, with few if any interfingering relationships observed.

Structures in the Black Hill quadrangle are indicative of regional extensional tectonics observed throughout the Rio Grande rift. A series of normal faults in the southwestern quadrangle are responsible for the volcanic and Paleozoic carbonate bedrock hills there and have an average strike of approximately 007°. In the northeastern map area, several faults striking approximately 345° form scarps up to 4-4.5 m high on the aggradational surface of the Palomas Formation as well as local erosional surfaces and middle Pleistocene terrace deposits near Crawford Hollow and Silver Canyon. These include the Black Hill fault crossing Interstate 25 north of Silver Canyon. The faults are probably 130-800 ka in age and have very low slip rates (<0.05 mm/yr).

INTRODUCTION

This report accompanies the Geologic Map of the Black Hill 7.5-Minute Quadrangle, Socorro County, New Mexico (NMBGMR OF-GM 274). Its purpose is to discuss the geologic setting and history of this area, and to identify and explain significant stratigraphic and structural relationships uncovered during the course of mapping.

The Black Hill 7.5-minute quadrangle is located in the southern part of the San Marcial Basin, an east-tilted half graben in the southern Rio Grande rift. It is bordered on the west by foothills of the southeastern San Mateo Mountains and is characterized by valleys of modest to considerable relief carved by east- or southeast-flowing tributaries to the Rio Grande. These drainages mostly head in the San Mateo Mountains or their foothills except for smaller washes such as Lumbre Canyon, which begins in the northwestern part of the quadrangle. From north to south, the major drainages of the quadrangle are Sheep Canyon, Lumbre Canyon, Crawford Hollow, Silver Canyon, Nogal Canyon, and Chaunte Canyon. Nogal Canyon forms an impressive gorge crossed by Interstate 25 and features local relief of up to 185 m where it runs adjacent to bedrock hills in the western quadrangle. The highest location in the quadrangle is 1738 m (5702 ft) above sea level (asl) at VABM Glorietta (13S 292590 mE, 3715082 mN NAD83). The lowest point is 1359 m (4459 ft) asl where a small wash exits the quadrangle between Nogal and Silver Canyons (13S 302530 mE, 3708882 mN NAD83).

The Black Hill quadrangle has an arid to semiarid climate. The summer months (June through August) experience mean temperatures of 23.6-25.6 °C (74.4-78.1 °F). The winter months (December through February) experience mean temperatures of 3.2-6.1 °C (37.8-43.0 °F). Mean annual precipitation is 25.1-25.9 cm (9.9-10.2 in), approximately half of which falls during the North American monsoon in the months of July through September. Climate data are from the Bosque del Apache and Rienhardt Ranch stations (ID# 291138 and 297423, respectively) in the NWS Cooperative network and averaged over the years 1981-2010 (Western Regional Climate Center, 2019).

The geology of the Black Hill quadrangle was previously mapped at 1:200,000-scale by Osburn (1984). Surrounding quadrangles mapped at a scale of 1:24,000 include the Romero Canyon quadrangle to the south (Cikoski, 2018) and a small portion of San Juan Peak to the northwest (Ferguson, 1986). The Paraje Well quadrangle to the east is currently being mapped at 1:24,000 by the New Mexico Bureau of Geology & Mineral Resources as part of its STATEMAP program.

This report includes a summary of the geologic setting before describing mapped units and their depositional settings by age, oldest to youngest. The structural geology of the area is briefly discussed, as are hydrogeologic implications for mapped basin-fill units. Detailed unit descriptions, $^{40}Ar/^{39}Ar$ age data, clast count data, maximum clast size, and paleocurrent measurements are provided as appendices.

GEOLOGIC SETTING

The Black Hill quadrangle is located in the southern Rio Grande rift, a series of en echelon basins stretching from northern Colorado to northern Mexico (Chapin and Cather, 1994). The quadrangle includes the southern part of the San Marcial Basin, an east- to southeast-tilted half-graben containing Miocene through early Pleistocene basin fill of the Santa Fe Group. Unlike the neighboring Engle Basin to the south, the San Marcial Basin lacks an obvious footwall-bounding uplift. Its (south)eastward tilt is inferred from stratigraphic dips and its half-graben geometry is inferred from Bouguer gravity anomaly data that implies an abrupt north-northeast-trending boundary between the San Marcial and Jornada del Muerto Basins (Keller, 1983; Kucks et al., 2001). Range-bounding faults to the north and south support this interpretation (Geddes, 1963; Nelson, 1986), as does a comparatively thinner package of Santa Fe Group basin fill underlying the western Jornada del Muerto Basin (Kelley, 1952).

The San Marcial Basin is bordered on the north and west by the Magdalena and San Mateo Mountains, both comprised chiefly of Paleogene volcanic rocks of the eastern Mogollon-Datil volcanic field with lesser proportions of intrusive bodies and Paleozoic sedimentary lithologies. The southeast San Mateo Mountains are the source area for most of the large drainages in the Black Hill quadrangle, contributing bedload clasts of felsic tuffs, flows, and intrusive rocks.

Prominent hills and low ridges in the southwest part of the map area are cored by Paleogene volcanic and Paleozoic carbonate rocks, uplifted along normal faults inferred to relate to one or more phases of Rio Grande rift extension beginning in the early Miocene. Other hills in the central quadrangle are formed of volcanic lithologies, including the eponymous Black Hill just east of New Mexico Highway 1. These features are uplifted along buried faults or faults with subtle surface expression and resemble erosional inselbergs.

Lower to middle Santa Fe Group basin-fill units exposed in Nogal Canyon record earlier phases of extension in the Rio Grande rift. These strata lie in both depositional and fault contact with Paleozoic carbonates and Eocene-Oligocene volcanic units, and appear to have filled in paleotopographic relief formed on the latter rocks west of Highway 1. The Santa Fe Group strata predating the Palomas Formation may be in part correlative to the middle to upper Miocene Rincon Valley Formation of the Palomas and Hatch-Rincon Basins to the south (Hawley et al., 1969; Seager et al., 1971).

Plio-Pleistocene basin fill of the Palomas Formation (upper Santa Fe Group) overlies the lower to middle Miocene deposits with angular unconformity. Named by early workers for extensive gravelly units in the Palomas Basin (Gordon and Graton, 1907; Gordon, 1910; Harley 1934) and formally defined by Lozinsky and Hawley (1986a, b), the Palomas Formation underlies most of the land surface of the Black Hill quadrangle. Six conformable, member-rank units can differentiated by color, texture, clast lithology, and degree of cementation.

The Palomas Formation piedmont facies units were deposited on hanging-wall distributary fan systems emanating from the foothills of the southeastern San Mateo Mountains, including a large paleofan of Nogal Canyon. Proximal through distal fan lithofacies are all represented among the Palomas piedmont units. Distal piedmont lithofacies interfinger with sandy beds containing pebbles of extra-basin lithologies (quartzite, granite, and chert) along the eastern quadrangle boundary. These represent axial-fluvial lithofacies deposited in braided channels or floodplain environments of an ancestral Rio Grande that integrated to southern New Mexico ~5 Ma (Mack et al., 2006; Koning et al. 2016, 2018).

The surface of the Nogal Canyon paleofan represents the local culmination of deposition of Palomas Formation basin fill, predating incision by the Rio Grande and its tributaries beginning in the middle Pleistocene. Aggradational geomorphic surfaces on lower Pleistocene basin fill in the Rio Grande rift vary somewhat in age but they generally date to ~0.8 Ma (Mack et al., 1993, 1998). Assuming the Nogal Canyon paleofan surface has a similar age, it is correlative to the Cuchillo surface of the Palomas and Engle Basins (Lozinsky, 1986; Lozinsky and Hawley, 1986a, b; Maxwell and Oakman, 1990; McCraw and Love, 2012) and the Las Cañas and Sedillo Hill surfaces of the Socorro Basin (McGrath and Hawley, 1987). North of Crawford Hollow, five erosional surfaces cutting the top of the Palomas Formation can be identified and inset middle-late Pleistocene and Holocene deposits are found throughout most drainages crossing the map area. The inset deposits indicate at least 4-6 alternating intervals of backfilling and incision.

METHODS

Geologic mapping of the Black Hill quadrangle involved traditional field techniques (Compton, 1985) coupled with newer digital approaches. Stereogrammetry software (Stereo Analyst for ArcGIS 10.1, an ERDAS extension, version 11.0.6) permitted accurate placement of geologic contacts using aerial photography obtained from the National Agricultural Imagery Program (NAIP). Planimetric and vertical accuracy of this dataset is approximately 5 m (USDA, 2008). Contacts plotted using stereogrammetry were then field-checked.

Descriptions of individual units were made in the field utilizing both visual and quantitative estimates based on outcrop and hand lens inspection. For clastic sediments, grain sizes follow the Udden-Wentworth scale and the term "clast(s)" refers to the grain size fraction greater than 2 mm in diameter (Udden, 1914; Wentworth, 1922). Carbonate rocks are classified according to Dunham (1962). Descriptions of bedding thickness follow Ingram (1954). Colors of sediment are based on visual comparison of dry samples to Munsell soil color charts (Munsell Color, 2009).

For volcanic units, grain or phenocryst size was described following the conventions of Wentworth (1922), Fisher (1961), and White and Houghton (2006). Color was estimated visually on both fresh and weathered surfaces. Other textural terms were assigned according to definitions in Winter (2010, p. 49-52).

Surface characteristics and relative landscape position were used in mapping middle Pleistocene to Holocene stream-terrace, alluvial-fan, and valley-floor deposits. Surface characteristics dependent on age include desert pavement development, clast varnish, soil development, and preservation of original bar-and-swale topography. Soil horizon designations and descriptive terms follow those of Birkeland and others (1991), Birkeland (1999), and Soil Survey Staff (1999). Stages of pedogenic calcium carbonate morphology follow those of Gile and others (1966) and Birkeland (1999).

STRATIGRAPHY

Paleozoic Rocks

Paleozoic carbonates (Pu) are exposed in several hills south of Nogal Canyon as well as sparse outcrops in the northwest quadrangle. The northernmost of these (13S 291315 mE, 3721845 mN NAD83) can be physically traced to the Paleozoic section at Bell Hill in the Steel Hill 7.5-minute quadrangle to the west. Kottlowski (1960) mapped this exposure as Pennsylvanian in age with Desmoinesian to Missourian fusulinids, although his stratigraphic section contains several discontinuities among marker fossils. Lucas et al. (2017) measured four sections near Bell Hill, none of which cross the small outcrop on the Black Hill quadrangle. However, the outcrop appears to correlate to the lower part of their section A1 on the upthrown side of a NE-trending fault. If correct, this correlation implies that the outcrop on the Black Hill quadrangle consists of limestones and perhaps fine-grained sandstone belonging to the Atokan Red House and Desmoinesian Gray Mesa Formations (Lucas et al., 2017).

Two hills underlain by limestone with minor covered intervals were mapped along Nogal Canyon near the western quadrangle boundary. The smaller hill at 13S 291360 mE, 3714799 mN NAD83 was not physically surveyed due to land access restrictions; it was vantage-mapped in the field and compared to the larger hill to the east using high-resolution aerial imagery. The larger hill is underlain by a succession of medium to dark gray, non- to occasionally cherty mudstone, wackestone, and packstone with fossils of nautiloids, bivalves, echinoderms, and sponge spicules. Some beds contain oval-shaped grains up to 3.5 mm long that are nearly always recrystallized but inferred to be fusulinids. Covered intervals are mostly underlain by shale. The lack of siliciclastic beds and fossil assemblages suggest a marine-shelf depositional environment (Lucas et al., 2012, 2016; Nelson et al., 2013). The Pennsylvanian section at Bell Hill is at least 495 m thick (Lucas et al., 2017), but <240 m is exposed in the Black Hill quadrangle at Nogal Canyon.

Osburn (1984) mapped the Nogal Canyon exposures as Permian in age but his map does not include discussion of this designation. Kottlowski (1960, p. 42) and Farkas (1969, p. 9) assign a Pennsylvanian age to the rocks in and along Nogal Canyon based on lithologic similarities to Kottlowski's section at Bell Hill. Indeed, the section of carbonate rocks at 13S 292400 mE, 3714410 mN NAD83 consists of ledge-forming, cherty, medium-bedded packstone and wackestone similar to the Elephant Butte and Whiskey Canyon Members of the Gray Formation as described by Lucas et al. (2017, p. 267); carbonate conglomerate of the overlying Garcia Member was not observed. Additionally, no siliciclastic red beds of the Permian Abo Formation as described at

Bell Hill (Kottlowski, 1960; Furlow, 1965; Lucas et al., 2017) are found at Nogal Canyon. Thus, we prefer the interpretation that these strata are Pennsylvanian in age.

Paleogene Volcanic Rocks

Four extrusive volcanic units are mapped on the Black Hill quadrangle as well as a volcaniclastic unit and an undivided volcanic unit (Tvu). The extrusive units include a trachyandesite, Tuff of Rocque Ramos Canyon, La Jencia Tuff, and Vicks Peak Tuff, each erupted from volcanic centers of the Mogollon-Datil volcanic field (Chapin et al., 1978, 2004; Elston, 1989). These units are upper Eocene to lower Oligocene in age; the Vicks Peak and La Jencia tuffs belong to the 29-24 Ma Mogollon Group and the Tuff of Rocque Ramos Canyon and trachyandesite belong to the 39-32 Ma Datil Group (Cather et al., 1994). Note that reported $^{40}Ar/^{39}Ar$ ages are calculated using a revised sanidine monitor age of 28.201 Ma for the Fish Canyon Tuff as advocated by Kuiper et al. (2008).

A trachyandesite (Tta) unconformably(?) underlies the Tuff of Rocque Ramos Canyon on a small hill south of Nogal Canyon (13S 293135 mE, 3713448 mN NAD83). Its contact with the carbonate strata to the west is inferred to occur along a buried SE-down structure; assuming the limestones are lower to middle Pennsylvanian in age, a fault is required to explain at least several hundred meters of missing upper Paleozoic (mostly Permian) and Eocene volcanic and volcaniclastic rocks (e.g., Spears Group). The trachyandesite consists of purplish brown, vesicular, massive to moderately flow-foliated, aphanitic lava with sparse phenocrysts of plagioclase and pyroxene with perhaps trace hornblende and olivine(?). Whole-rock geochemistry of the unit returned SiO_2 and $Na_2O + K_2O$ values of 59.2 and 9.9 wt %, respectively (Table 1). Its geochemistry is similar to the Luna Peak (trachy)andesite of the Red Rock Ranch Formation in the Monticello area (Koning et al., 2014), but its phenocryst content is more akin to the overlying Red Rock Arroyo andesite. The Red Rock Ranch Formation is upper Eocene in age (Farkas, 1969; Hermann, 1986; Koning et al., 2014). Ferguson (1986) described a basaltic andesite similar in appearance to the trachyandesite in the east-central San Mateo Mountains; however, he speculates that the unexposed base of this andesite lies above the 32.0 Ma Hells Mesa Tuff (Ferguson, 1988, p. 4) so correlation between the two units is doubtful. The exposed thickness of the trachyandesite in the map area is 65-70 m.

The Tuff of Rocque [*sic*] Ramos Canyon (Trr) was named by Harrison (1990) for exposures in Roque Ramos Canyon in the eastern Sierra Cuchillo ~35 km southwest of the map area. It is found at Black Hill and a series of low hills to its west as well as underlying the Vicks Peak (and, locally, La Jencia) tuffs south of Nogal Canyon. The Tuff of Rocque Ramos Canyon is a light-gray to white or pinkish-gray to reddish-brown, moderately to densely welded ash-flow tuff. Cikoski et al. (2010) describe an upper, moderately welded unit with <7% phenocrysts and a lower, densely welded unit with 15-20% phenocrysts (mostly sanidine) in the Indian Well Wilderness 7.5-minute quadrangle 30-35 km northeast of the map area. In tandem, these units are up to 60 m thick. In the Black Hill quadrangle, phenocrysts occupy 15-40% of the surface area and are composed mainly of fine to medium sanidine with subordinate plagioclase and trace to 7% biotite, the latter commonly with coppery luster. Whole-rock geochemistry suggests that the unit is trachytic to rhyolitic with SiO_2 and $Na_2O + K_2O$ values of 68.7 and 10.5 wt %, respectively (Table 1). Harrison (1990) noted similar geochemistry in the northern Black Range. The unit contains 1-5% pumice that are 1-10 cm long and relatively undeformed to highly flattened; occasional compaction foliation is more poorly developed than that of the La Jencia Tuff. At Black Hill, <10-15% pebble-sized lithic andesite fragments are present. South of Nogal Canyon, the unit includes a reddish-brown, ledge-forming, volcaniclastic facies underlying welded, sanidine-rich tuff. These facies have a mostly matrix-supported texture with subangular to subrounded, pebble-sized pumice and minor aphanitic andesite clasts. Cikoski et al. (2010) reported an average $^{40}Ar/^{39}Ar$ age of 35.75 ± 0.01 Ma and 35.72 ± 0.01 Ma were obtained for the Tuff of Rocque Ramos Canyon in the Black Hill quadrangle (Appendix B). The unit has been correlated with the Bell Top 4 tuff (McIntosh et al., 1991), for which Clemons (1975) suggested a source area in the Sierra de las Uvas near Hatch, New Mexico. However, McIntosh (1989) suggested that the Emory caldera of the more proximal Black Range may be the source of the Tuff of Rocque Ramos Canyon; no definitive source caldera has yet been identified. The tuff is <80-100 m thick in the Black Hill quadrangle.

A thin (<7-10 m) bed of the La Jencia Tuff (Tlj) underlies the Vicks Peak Tuff in the southwestern corner of the quadrangle (13S 293845 mE, 3709950 mN NAD83). The bed consists of purplish-brown to gray, welded, rhyolitic ash-flow tuff with 2-8% phenocrysts of fine to medium

Table 1. Major-element geochemistry of extrusive rocks in the Black Hill 7.5'

Sample ID	18BH-724	18BH-740	18BH-749	19BH-565
	La Jencia Tuff	Vicks Peak Tuff	Tuff of Rocque Ramos Canyon	Trachyandesite
Map Unit	Tlj	Tvp	Trr	Tta
Al_2O_3	14.85	11.61	15.15	16.69
BaO	0.04	0.03	0.09	0.20
CaO	0.60	0.08	1.34	3.72
Cr_2O_3	<0.01	<0.01	<0.01	<0.01
Fe_2O_3	2.25	1.70	2.02	5.30
K_2O	5.63	4.73	5.90	5.22
MgO	0.30	0.13	0.46	1.17
MnO	0.07	0.08	0.08	0.09
Na_2O	5.01	4.39	4.62	4.70
P_2O_5	0.08	0.04	0.12	0.53
SO_3	0.02	<0.01	0.04	0.17
SiO_2	69.87	75.89	68.74	59.16
SrO	0.01	<0.01	0.01	0.07
TiO_2	0.45	0.20	0.43	1.38
LOI	0.36	0.02	0.54	1.83
Total	99.65	98.99	99.63	100.35

NOTE: Oxide analysis by X-ray fluorescence, ALS USA, Inc. LOI = loss on ignition. All reported values are wt %.

sanidine and biotite. Brown (1972) notes that outflow facies of the La Jencia (his "lower tuff of Bear Springs") may also contain smoky quartz and plagioclase crystals as well as andesitic to rhyolitic lithics; a few altered lithics are observed in the limited exposures of the map area. Whole-rock SiO_2 and $Na_2O + K_2O$ contents are 69.9 and 10.6 wt %, respectively (Table 1). Abundant fiamme and stretched vesicles and lapilli exhibit highly variable length:width ratios, ranging from 3:1 to 76:1. The La Jencia Tuff was erupted from the Sawmill Canyon caldera in the Magdalena Mountains ~40 km north of the Black Hill quadrangle (Osburn and Chapin, 1983; Chapin et al., 2004). Given its limited spatial extent, the La Jencia Tuff in the map area is inferred to have filled a paleotopographic low formed on the Tuff of Rocque Ramos Canyon. An $^{40}Ar/^{39}Ar$ age of 29.00 ± 0.02 Ma was obtained (Appendix B), closely matching previously reported ages (McIntosh et al., 1991; Chapin et al., 2004).

Named by Farkas (1969) for exposures in the nearby San Mateo Mountains, the Vicks Peak Tuff (Tvp) is one of the most extensive tuff units erupted from the northeastern Mogollon-Datil field (McIntosh et al., 1992). It comprises most of the hills west of Highway 1 in the southwest part of the quadrangle and is also found atop a small knoll west of Black Hill. In most places on the quadrangle, the Vicks Peak overlies the Tuff of Rocque Ramos Canyon, representing an unconformity of nearly 7 million years. The Vicks Peak overlies a thin (<6 m), poorly exposed bed of volcaniclastic sediment (Tvs) west of Black Hill; this deposit lies atop the Tuff of Rocque Ramos Canyon.

In the Black Hill quadrangle, the Vicks Peak Tuff is a light-gray, occasionally columnar-jointed, crystal-poor, rhyolitic ash-flow tuff. Phenocrysts include trace to 3% sanidine, trace to 1% mafics, and trace quartz set in a devitrified matrix. Whole-rock SiO_2 and $Na_2O + K_2O$ contents are 75.9 and 9.1 wt %, respectively (Table 1).

The tuff exhibits occasional eutaxitic foliation and sparse to abundant spherulites. A dark-gray to black vitrophyre is commonly observed at the base of the Vicks Peak in the southern part of the map area. An $^{40}Ar/^{39}Ar$ age of 28.72 ± 0.02 Ma was obtained (Appendix B). The Vicks Peak Tuff is up to 180 m thick in the southern quadrangle. Its relatively high thickness here is no doubt due to its proximity (<6-8 km) to its source, the Nogal Canyon caldera (Hermann, 1986; Lynch, 2003). The lack of collapse breccias and rhyolitic intrusions and domes observed several km to the west (Atwood, 1982) indicate that the Vicks Peak Tuff in the quadrangle is comprised entirely of outflow facies.

Early Pleistocene-Miocene Basin Fill

Basins throughout the Rio Grande rift are characterized by thick accumulations of clastic sediment (with minor interbedded volcanic deposits) collectively known as the Santa Fe Group (e.g., Kelley, 1977; Hawley, 1978; Gile et al., 1981; Chapin and Cather, 1994; Connell, 2008). This sediment was deposited during Rio Grande rift extension. Basin-fill packages vary in age depending on location but generally span the early Miocene through early Pleistocene. Plio-Pleistocene and Miocene basin-fill deposits underlie much of the Black Hill quadrangle.

Basin fill of a mostly fine-grained nature that is inferred to be Miocene in age is found along Nogal Canyon in its deeper reaches near the western margin of the quadrangle. These sediments were not studied in detail due to land access restrictions, but their yellowish to reddish-brown colors and locally strong cementation (limited to conglomerates and coarse sandstones) are reminiscent of lower to middle Miocene sediment mapped in the Palomas Basin to the south (Jochems, 2015; Koning et al., 2015; Jochems and Koning, 2017; Jochems and Cox, 2019). Thus, we correlate the Nogal Canyon sediments to piedmont facies of the lower and middle Santa Fe Group (Tsml) predating the Palomas Formation. In the Truth or Consequences area and western Palomas Basin, basin fill in a similar stratigraphic position has been correlated in part to the middle to upper Miocene Rincon Valley Formation of Hawley et al. (1969) and Seager et al. (1971) (Koning et al., 2016; Jochems and Koning, 2017). Miocene basin fill in the rift was deposited prior to integration of the ancestral Rio Grande to southern New Mexico and typically consists of coarser piedmont facies transitioning to finer-grained facies that filled closed basins (e.g., Mack et al., 1994; Connell, 2008). The lower to middle Santa Fe Group on the Black Hill quadrangle is at least 90 to perhaps 100s of meters thick but sparse well control and a lack of high-resolution geophysical data prohibit an accurate estimate.

Plio-Pleistocene gravel, sand, silt, and clay belonging to the Palomas Formation (upper Santa Fe Group) lies above the older basin fill in the map area, attaining a minimum thickness of 180 m. The term "Palomas" was first applied to outcrops of upper Santa Fe Group basin fill by Gordon and Graton (1907), Gordon (1910), and Harley (1934). Gordon (1910, plate XII) used the term for surficial sediments throughout the Engle, Jornada del Muerto, Palomas, and San Marcial Basins. Lozinsky and Hawley (1986a) formally defined the Palomas Formation and detailed descriptions of the unit are presented in Lozinsky and Hawley (1986a, b) and Lozinsky (1986). Fossil data (summarized by Morgan and Lucas, 2012), radiometric ages (Bachman and Mehnert, 1978; Seager et al., 1984; Jochems, 2015; Koning et al., 2015, 2016, 2018), and magnetostratigraphic data (Repenning and May, 1986; Mack et al., 1993, 1998) indicate an age range of ~5.0-0.8 Ma for the Palomas Formation.

The Palomas Formation is divided into six conformable, member-rank units on the Black Hill quadrangle. The lower piedmont facies (Tppl) consists of 35-45 m of grayish, variably consolidated gravel/conglomerate containing pebbles through boulders of dominantly felsic lithologies, including up to 50% Vicks Peak Tuff (Appendix B). The unit is best exposed in low-lying ridges of the southwestern quadrangle where it onlaps the Vicks Peak Tuff, the latter forming an apparent paleotopographic high. Vantage and aerial imagery mapping indicate that the lower piedmont facies lies with angular unconformity on strongly cemented lower-middle Santa Fe Group in Nogal Canyon. A similar relationship is observed in parts of the western Palomas Basin, although the contact is typically gradational at basinward locations (Koning et al., 2015; Jochems and Koning, 2017; Jochems and Cox, 2019). The lower piedmont facies is interpreted as having been deposited by debris flows in proximal alluvial fan settings.

The undivided lower to middle piedmont facies (QTppml) was mapped in parts of Nogal Canyon not accessed due to land permission restrictions, but it probably consists of <60 m of silty or sandy sediment and gravel that may coarsen to the west. The middle piedmont facies (QTppm), well-exposed in Nogal Canyon and between

Silver Canyon and Crawford Hollow, is dominated by reddish to pinkish or pale brown (5YR 5-6/4; 7.5YR 7/3-4, 6/3-4; 10YR 7/3-4), extra-channel silt and mud with subordinate fluvial or debris-flow sand and gravels and minor calcareous *ciénega* (marsh) deposits found at distal fan positions in the eastern quadrangle. Channel-fill gravels are distinctly lenticular and typically less than several 10s of meters in profile; these commonly represent smaller side channels spilling out onto alluvial flats or perhaps the floodplains of larger trunk drainages. Buried calcic soils (stage I-III carbonate morphology; Gile et al., 1966) are sometimes found in finer-grained deposits. These are distinguished from *ciénega* deposits by gradual contacts, ped development, and association with illuviated clay horizons (Mack et al., 2000). Where preserved, paleosols indicate periods of landscape stability, likely on interfluves lying above actively depositing channels or lobes of distributive fan systems. The middle piedmont facies have a maximum thickness of at least 60 m. A lateral transition from the middle piedmont facies in the west to sandy axial-fluvial facies in the east is readily identified in Nogal Canyon.

The upper piedmont facies (Qppu) includes interbedded gravel bodies, pebbly silt-sand, silt, and mud with a maximum thickness of 85 m. This unit consists almost entirely of stacked gravel deposits deposited by debris flows in Nogal Canyon near and upstream of Interstate 25. Gravels occur in sheet-like to lenticular bodies that are nearly always imbricated to some extent (average measured paleocurrent = 113°, n = 68; Appendix D). Occasional cross-stratification and lateral accretion sets attest to deposition in channel systems but tabular, non-crossbedded geometries are more common. Clast lithologies are mostly fine-grained felsic volcanics (Appendix C), but subtle changes in the proportion of certain lithologies help to delineate specific source areas in the eastern San Mateo Mountains. For example, intermediate volcanic clasts increase from north to south (<1% in the north to <15% south of Crawford Hollow) and relatively crystal-rich (>3%) felsites are limited to areas in the paleo-Nogal-Silver Canyon drainage. The upper piedmont facies contains <50% gravels east of Interstate 25, where it is distinguished from the middle piedmont unit by redder colors (5YR 5-6/3-4 or 4-6/6; 7.5YR 6/6) due to a greater proportion of matrix clay, in addition to more common sheet-like geometries among its gravel beds. Buried calcic horizons are less common than in the middle piedmont facies, although the upper piedmont unit is frequently capped by soils with stage III-III+ carbonate accumulation, particularly around Nogal Canyon. Illuviated clay horizons are apparently more common among buried soils in finer-grained deposits of the upper piedmont facies. In most of the quadrangle, the upper piedmont facies has prograded over the middle piedmont and axial-fluvial facies, with few if any interfingering relationships observed. Given a biostratigraphic age constraint for the axial-fluvial facies (see below), the upper piedmont facies must be entirely early Pleistocene in age.

The upper piedmont facies of the Palomas Formation in the southern two-thirds of the quadrangle underlies a large paleofan with a northern margin near Crawford Hollow. This feature, at least 8 km across, is evidently responsible for the modern, fanning topography in the central and southern parts of the quadrangle. Modern Nogal Canyon apparently runs south of the main axis because the north-south profile of the fan is convex with its highest point located between Black Hill and Silver Canyon. The Palomas Formation underlying the Nogal Canyon paleofan exhibits an upward coarsening trend similar to that observed in the Palomas Basin (Grundwald, 1990; Jochems and Koning, 2015a; Koning et al., 2015). Clearly, the paleo-Nogal-Silver Canyon drainage had become a high-competency system by the early Pleistocene; paleoclimatic factors favoring low sediment/water ratios may have led to increased contributions of sediment over time. Coarsening trends among other basin-fill packages in New Mexico have been also been ascribed to paleoclimatic drivers (e.g., Koning et al., 2002). The Nogal Canyon paleofan was likely a distributive fan system (Weissmann et al., 2010) throughout the history of Palomas Formation deposition, given that large precursor channel systems to modern Nogal and Silver Canyons appear to have migrated freely across its surface.

The axial-fluvial facies of the Palomas Formation (QTpa) consists mainly of fine- to coarse-grained, quartzose sand with subordinate gypsiferous mud and pebble gravel beds, the latter containing extra-basin clast lithologies such as chert, granite, and quartzite (Appendix C). Common cross-stratification represents a variety of bar structures, including linguoid or transverse bars nearly orthogonal to south-southeast or south-southwest paleocurrent directions determined from clast imbrication (164-196°; Appendix D). These structures along with minimal proportions of mud suggest deposition in a braided channel system of the ancestral Rio Grande. Vertebrate fossils recovered from channel-margin deposits of the

axial-fluvial facies include a horse (*Equus* sp.), packrat (*Neotoma* sp.), a glyptodont (*Glyptotherium* sp.), and teeth of an unidentified gomphotheriid proboscidean (Morgan and Lucas, 2003, p. 292; G. Morgan, pers. comm., 2019). These fossils indicate a Blancan age for the unit, with its top younger than ~2.7 Ma. A thin, fine-grained subunit (QTpaf) found in Crawford Hollow consisting of massive mud represents floodplain deposition and interfingers with the middle piedmont facies. The total thickness of the axial-fluvial facies is unknown but projections of contacts from cross-section A-A' and well data indicate a minimum thickness of 70-75 m in the Silver Canyon area.

Quaternary Deposits (Post-Palomas Formation)

Deposition of the Palomas Formation in the Black Hill quadrangle probably ended ~0.8 Ma, assuming that the surface of the Nogal Canyon paleofan is similar in age to other constructional surfaces in the southern Rio Grande rift (Mack et al., 1993, 1998). By the middle Pleistocene, the Rio Grande and its tributaries had begun incising to eventually form the modern network of arroyos and stream valleys. Valley-margin deposits include inset stream terraces. Valley-floor deposits include low-lying terraces adjacent to modern stream courses and young (Holocene) alluvial fans.

As many as six middle to late Pleistocene terraces are found along the valley margins of drainages crossing the Black Hill quadrangle. Terrace gravels are generally strath deposits <4 m thick, but fill terrace gravels up to 12 m thick are found along Crawford Hollow (Qtc4) and Silver Canyon (Qts4), particularly at downstream positions. These deposits are inferred to be middle Pleistocene in age based on their landscape position. The Silver Canyon deposit is particularly noteworthy because it is the only pre-Holocene deposit observed in that drainage in the map area. Clearly, Silver Canyon experienced stream capture by Nogal Canyon after deposition of Qts4 gravels. This event apparently occurred ~1.5 km upstream of the western quadrangle boundary (near 13S 289695 mE, 3716855 mN NAD83). By the late Pleistocene, headward migration of incision in Silver Canyon was occurring between the eastern quadrangle boundary and the Rio Grande floodplain, as evidenced by younger (probably late Pleistocene) terrace deposits on the Paraje Well 7.5-minute quadrangle to the east. A minor amount of vertical incision has occurred during the late Pleistocene and Holocene throughout much of the Silver Canyon drainage.

In addition to their inset positions, terrace deposits are distinguished from gravelly sediment of the Palomas Formation by browner colors (e.g., 7.5YR 4-6/4-6), poorer sorting, poorer consolidation, and a lack of buried soils. Older terrace surfaces (treads) may feature moderate desert pavement, moderate to strong varnish on up to 65% of clasts, and topsoils with illuviated clay horizons and calcic soils with up to stage IV carbonate accumulation. Terrace treads tend to diverge in a downstream direction (i.e. to the east) in most drainages. Tread elevations in Nogal Canyon vary from 7 to 73 m above the modern valley floor (typically Qah surfaces). Thus, Nogal Canyon has incised at an "average" rate of ~90 m/myr since the middle Pleistocene. This rate is similar to an estimate of 70 m/myr for a Rio Grande terrace containing the 640 ka Lava Creek B ash near Truth or Consequences (Jochems and Koning, 2015a). However, these estimates do not take into account the dynamic shifting of baselevel over time (Gallen et al., 2015) nor do they integrate the ages and elevations of younger, undated terrace deposits.

Valley-floor deposits that postdate terrace gravels include younger and historical alluvium that is mostly Holocene in age. Younger alluvium (Qay) consists of brownish (5-10YR), gravelly sand and pebbly gravel underlying low terraces adjoining active channels or relatively inactive valley floors. These deposits have topsoils with illuviated clay (Bt) and calcic horizons with stage I to II carbonate accumulation. They are distinguished from historical alluvium (Qah) by soil development, tread height, and a lack of bar-and-swale relief on their treads. Historical alluvium consists of yellowish-brown or brown (7.5-10YR) sand and gravel with little to no clay illuviation in the topsoil. Maximum tread heights for Qay and Qah deposits are 2.5 and 1.5 m above modern grade, respectively. Alluvial fans graded to these deposits typically have similar colors, soil development, and bar-and-swale relief but may be coarser, more poorly sorted, and tabular to wedge-shaped.

In general, middle to late Pleistocene deposits in the Black Hill quadrangle and throughout the Rio Grande rift formed during periods of climatic fluctuation related to glacial-interglacial cycles. One model proposes that terrace formation in the southern Rio Grande rift occurs in three stages: (1) the Rio Grande and the lower valleys of its tributaries incised during full glacial conditions; (2) aggradation occurred during the transition to interglacial intervals due to decreased water to sediment ratios; and (3) stability ensued for the remainder of the interglacial interval (Gile et al., 1981).

Holocene incision episodes inferred from radiocarbon ages of valley-floor deposits in the Palomas Basin indicate that down-cutting of arroyos may have occurred during periods of enhanced summer monsoon, whereas Rio Grande incision may have been more sensitive to winter precipitation in its headwaters (Mack et al., 2011; Jochems and Koning, 2015b). Incision during summer monsoons may be enhanced by overall arid climate due to sparser vegetation.

Erosional Surfaces

Five erosional surfaces (Qx2-6) are found north of Crawford Hollow, the most extensive of which are graded to intermediate or higher positions in the landscape (Qx4, Qx6). These surfaces have formed mostly on the upper piedmont facies of the Palomas Formation although a few occur on Crawford Hollow terrace deposits. The surfaces are nearly flat to slightly convex; maximum slopes are <2% and average slopes are commonly <0.5%. The erosional surfaces are seldom associated with underlying deposits. Only a young pediment in a tributary to Sheep Canyon (Qpw1) appears to overlie a 2-3 m thick deposit of silt, sand, and gravel not associated with other valley-floor deposits. Because the erosional surfaces are graded to similar positions as terrace gravels in the northern quadrangle, they are inferred to range from middle to late Pleistocene in age. Ferguson (1988) describes a pedimented surface extending from the foothills of the San Mateo Mountains in the Tenmile Hill 7.5-minute quadrangle ~20 km to the northwest, but its relation to the erosional surfaces in the map area is not constrained.

STRUCTURAL GEOLOGY

The Black Hill quadrangle is located at the southern end of the (south)east-tilted San Marcial Basin. A steep gravity gradient to the east of the map area is indicative of a poorly exposed footwall margin, but the quadrangle itself lies above a low-gradient, bench-like anomaly adjacent to steep gradients and high anomalies in the volcanic-cored San Mateo Mountains to the west (Keller, 1983).

Most structures in the Black Hill quadrangle are indicative of regional extensional tectonics observed throughout the Rio Grande rift. A series of normal faults in the southwestern quadrangle bound small footwall blocks cored by Paleogene volcanic or Paleozoic carbonate bedrock. These faults have an average strike of approximately 007°, with one southwest-down fault striking 310°. The northerly strike of the faults closely parallels the southeast margin of the Nogal Canyon caldera as delineated by Atwood (1982), Osburn and Chapin (1983), and Hermann (1986). That Pennsylvanian strata are the youngest pre-Cenozoic rocks in this area suggests that it was a topographic high during the Cretaceous-Eocene Laramide orogeny (R. Chamberlin, pers. comm., 2019).

In the northeastern map area, faults striking approximately 345° form scarps up to 4-4.5 m high on the aggradational surface of the Palomas Formation as well as local erosional surfaces and middle Pleistocene terrace deposits near Crawford Hollow and Silver Canyon. These include the Black Hill fault crossing Interstate 25 north of Silver Canyon which forms scarps up to 2 m higher than nearby faults. However, it does not appear that this fault deforms younger geomorphic surfaces than the others. The Black Hill fault may have been the basin-margin fault at one time, given the volcanic bedrock at Black Hill in its footwall; if so, the basin margin has clearly been dissected and retreated to the west (Machette and Jochems, 2016a). The remaining faults belong to the Milligan Gulch fault zone. All are probably 130-800 ka in age with slip rates of <0.05 mm/yr (Machette and Jochems, 2016a, b).

HYDROGEOLOGY

Aquifers of adequate quantity and quality for domestic, municipal, and agricultural use in surrounding basins are typically found in the Santa Fe Group and younger Quaternary valley-fill units. Based primarily on mapping in the Palomas Basin and comparison to units in the map area, we briefly describe the potential of basin-fill and valley-floor units of the Black Hill quadrangle for groundwater resources. Note that water may be also be transmitted through fractured bedrock units.

Santa Fe Group units predating the Palomas Formation commonly contain alluvial sands and gravels. However, the intrinsic permeability of these deposits is likely to be affected by matrix- versus clast-supported texture and cementation. For instance, lower to middle Santa Fe Group units in the Palomas Basin are often well-cemented by calcite or silica, potentially hindering groundwater flow, but cementation in these units likely decreases toward the east (Koning et al., 2015). A correlative unit in the Black Hill quadrangle (Tsml) could exhibit a similar pattern, with any groundwater present expected to be confined

to sand/sandstone or gravel/conglomerate beds that are bound by finer, muddy to silty beds. The sandy to gravelly beds could be productive, water-bearing units in the basin center, although hydrostratigraphic facies models predict that piedmont sands and gravels often transition laterally to finer-grained basin-floor facies lacking high-quality aquifers (e.g., Hawley and Whitworth, 1996).

The aquifer-hosting potential of the Palomas Formation is similarly predicated on texture and continuity of permeable beds, and perhaps cementation to a lesser extent. The upper piedmont facies lies above the water table in most places, but certain characteristics of the middle and lower piedmont facies could be favorable to permeability and transmissivity of groundwater. The lower piedmont facies is a dominantly gravelly deposit but calcite cementation could decrease permeability, particularly in proximal alluvial fan settings. Channel-fill gravels in the middle piedmont facies are seldom cemented and lack clay. Additionally, abundant silty to clayey beds in the unit could act as aquitards, confining groundwater to the channel fills. Thus, gravels in the middle piedmont facies could host groundwater as they are thought to do in the Palomas Basin (Jochems and Koning, 2015a, 2017), the primary limitation being their lateral continuity. Finally, the sandy, non-cemented axial-fluvial facies are likely to serve as a high-quality aquifer, although the lack of extensive clayey floodplain deposits could result in excessive leakage (Davie and Spiegel, 1967). Plio-Pleistocene axial-fluvial sediment has been a significant source of groundwater in other basins of the Rio Grande rift (e.g., Hawley and Whitworth, 1996; Hawley et al., 2009).

Holocene valley-floor units may also locally host aquifers. Gravelly or sandy channel fills in historical and younger alluvium could be saturated in places where they underlie modern floodplains. Elsewhere, coarse valley-floor units transmit runoff, mostly during the summer months of the monsoon season, to underlying Palomas Formation aquifers. Alternatively, they may locally receive groundwater discharge from buried basin-fill aquifers (Davie and Spiegel, 1967), although this scenario seems limited to the floor of the deeply cut Nogal Canyon in the western map area where vegetation becomes more abundant. It is also likely that a complex fault-fracture system transmits water to the surface in this area.

Water from basin-fill and valley-floor aquifers is generally of moderate to high quality, particularly in sparsely populated regions like the San Marcial Basin where anthropogenic pollution sources are less common. Land (2016) analyzed 32 well records for water quality in the Engle and San Marcial Basins. Median total-dissolved solids (TDS) were 456 mg/L, slightly below the EPA secondary standard of 500 mg/L. Median well depth was 300 ft, indicating that most sampled wells were probably completed in the lower or middle intervals of the Palomas Formation. Although most of the analyzed wells are in the Engle Basin, groundwater there shares a common source area/geology with the San Marcial Basin (San Mateo Mountains) and water quality is likely to be similar.

The San Marcial Basin is one of the least densely populated areas along the Rio Grande corridor in New Mexico and most wells are used for agricultural purposes (i.e. water for livestock). Thus, there is currently low potential for the development of groundwater resources in the map area. Future investigations of groundwater resources in the map area should focus on the lower and middle piedmont facies of the Palomas Formation, the axial-fluvial facies of the Palomas, and Holocene valley-floor units as these deposits are most likely to yield high quality water in significant amounts.

ACKNOWLEDGMENTS

Mapping of the Black Hill quadrangle was funded by the STATEMAP program, which is jointly supported by the U.S. Geological Survey and the New Mexico Bureau of Geology and Mineral Resources (NMBGMR). We thank Dr. J. Michael Timmons of NMBGMR for logistical support and coordination. Matt Heizler and Lisa Peters of the New Mexico Geochronology Research Laboratory provided $^{40}Ar/^{39}Ar$ ages for the La Jencia and Vicks Peak tuffs in the southern part of the quadrangle. Geochemical data for volcanic units were provided by ALS USA Inc.

REFERENCES

Atwood, G.W., 1982, Geology of the San Juan Peak area, San Mateo Mountains, Socorro County, New Mexico: with special reference to the geochemistry, mineralogy, and petrogenesis of an occurrence of riebeckite-bearing rhyolite [M.S. thesis]: Albuquerque, University of New Mexico, 168 p.

Bachman, G.O., and Mehnert, H.H., 1978, New K-Ar dates and the late Pliocene to Holocene geomorphic history of the Rio Grande region, New Mexico: Geological Society of America Bulletin, v. 89, p. 283–292.

Birkeland, P.W., 1999, Soils and geomorphology: Oxford, UK, Oxford University Press, 448 p.

Birkeland, P.W., Machette, M.N., and Haller, K.M., 1991, Soils as a tool for applied Quaternary geology: Utah Geological and Mineral Survey, Miscellaneous Publication 91–3, 63 p.

Brown, D.M., 1972, Geology of the southern Bear Mountains, Socorro County, New Mexico: New Mexico Bureau of Mines and Mineral Resources, Open-file Report 042, 109 p., 1 plate, scale 1:24,000.

Cather, S.M., Chamberlin, R.M., and Ratté, J.C., 1994, Tertiary stratigraphy and nomenclature for western New Mexico and eastern Arizona, *in* Chamberlin, R.M., Kues, B.S., Cather, S.M., Barker, J.M., and McIntosh, W.C., eds., Mogollon Slope, West-central New Mexico and East-central Arizona: New Mexico Geological Society, Guidebook 45, p. 259–266.

Chapin, C.E., and Cather, S.M., 1994, Tectonic setting of the axial basins of the northern and central Rio Grande rift, *in* Keller, G.R., and Cather, S.M., eds., Basins of the Rio Grande Rift: Structure, Stratigraphy, and Tectonic Setting: Geological Society of America, Special Paper 29, v. 291, p. 5–25.

Chapin, C.E., Elston, W.E., and James, H.L., eds., 1978, Field guide to selected cauldrons and mining districts of the Datil-Mogollon volcanic field, New Mexico: New Mexico Geological Society, Special Publication 7, 149 p.

Chapin, C.E., McIntosh, W.C., and Chamberlin, R.M., 2004, The late Eocene-Oligocene peak of Cenozoic volcanism in southwestern New Mexico, *in* Mack, G.H. and Giles, K.A., eds., The Geology of New Mexico: A Geologic History: New Mexico Geological Society, Special Publication 11, p. 271–293.

Cikoski, C.T., 2018, Geologic map of the Romero Canyon 7.5-minute quadrangle, Sierra and Socorro Counties, New Mexico: New Mexico Bureau of Geology and Mineral Resources, Open-File Geologic Map OF-GM 270, scale 1:24,000.

Cikoski, C.T., Chamberlin, R.M., Eggleston, T.L., Kent, S.C., and Lucas, S.G., 2010, Geologic map of the Indian Well Wilderness 7.5-minute quadrangle, Socorro County, New Mexico: New Mexico Bureau of Geology and Mineral Resources, Open-File Geologic Map OF-GM 201, scale 1:24,000.

Clemons, R.E., 1975, Petrology of the Bell Top Formation, *in* Seager, W.R., Clemons, R.E., and Callender, J.F., eds., Las Cruces Country: New Mexico Geological Society, Guidebook 26, p. 123–130.

Compton, R.R., 1985, Geology in the field: New York, John Wiley & Sons, 398 p.

Connell, S.D., 2008, Refinements to the stratigraphic nomenclature of the Santa Fe Group, northwestern Albuquerque Basin, New Mexico: New Mexico Geology, v. 30, p. 14–35.

Davie, W., Jr., and Spiegel, Z., 1967, Geology and water resources of Las Animas Creek and vicinity, Sierra County, New Mexico: New Mexico State Engineer Hydrographic Survey Report, 44 p.

Dunham, R.J., 1962, Classification of carbonate rocks according to depositional texture, *in* Ham, W.E., ed., Classification of Carbonate Rocks: American Association of Petroleum Geologists Memoir, p. 108–121.

Elston, W.E., 1989, Overview of the Mogollon-Datil volcanic field, *in* Chapin, C.E., and Zidek, J., eds., Field Excursions to Volcanic Terranes in the Western United States—Volume I, Southern Rocky Mountain Region: New Mexico Bureau of Mines and Mineral Resources, Memoir 46, p. 43–46.

Farkas, S.E., 1969, Geology of the southern San Mateo Mountains, Socorro and Sierra Counties, New Mexico [Ph.D. dissertation]: Albuquerque, University of New Mexico, 181 p.

Ferguson, C.A., 1986, Geology of the east-central San Mateo Mountains, Socorro County, New Mexico: New Mexico Bureau of Mines and Mineral Resources, Open-file Report 252, 124 p., 4 plates.

Ferguson, C.A., 1988, Geology of the Tenmile Hill 7.5' quadrangle, Socorro County, New Mexico: New Mexico Bureau of Mines and Mineral Resources, Open-file Report 283, 21 p., 2 plates, scale 1:24,000.

Fisher, R.V., 1961, Proposed classification of volcaniclastic sediments and rocks: Geological Society of America Bulletin, v. 72, p. 1409–1414.

Furlow, J.W., 1965, Geology of the San Mateo Peak area, Socorro County, New Mexico [M.S. thesis]: Albuquerque, University of New Mexico, 83 p.

Gallen, S.F., Pazzaglia, F.J., Wegmann, K.W., Pederson, J.L., and Gardner, T.W., 2015, The dynamic reference frame of rivers and apparent transience in incision rates: Geology, v. 43, p. 623–626, doi:10.1130/G36692.1.

Geddes, R.W., 1963, Structural geology of Little San Pasqual Mountain and the adjacent Rio Grande trough [M.S. thesis]: Socorro, New Mexico Institute of Mining and Technology, 62 p.

Gile, L.H., Peterson, F.F., and Grossman, R.B., 1966, Morphological and genetic sequences of carbonate accumulation in desert soils: Soil Science, v. 101, p. 347–360.

Gile, L.H., Hawley, J.W., and Grossman, R.B., 1981, Soils and geomorphology in the Basin and Range area of southern New Mexico—guidebook to the Desert Project: New Mexico Bureau of Mines and Mineral Resources, Memoir 39, 222 p.

Gordon, C.H., 1910, Sierra and central Socorro Counties, *in* Lindgren, W., Graton, L.C., and Gordon, C.H., eds., The Ore Deposits of New Mexico: U.S. Geological Survey Professional Paper 68, p. 213–285.

Gordon, C.H., and Graton, L.C., 1907, Lower Paleozoic formations in New Mexico (abstract): Journal of Geology, v. 15, p. 91–92.

Grundwald, T.W., 1990, Depositional environments and paleosols of the Palomas Formation (Plio-Pleistocene), Palomas Basin, southern Rio Grande rift [M.S. thesis]: Las Cruces, New Mexico State University, 95 p.

Harley, G.T., 1934, The geology and ore deposits of Sierra County, New Mexico: New Mexico Bureau of Mines and Mineral Resources, Bulletin 10, 220 p.

Harrison, R.W., 1990, Cenozoic stratigraphy, structure, and epithermal mineralization of north-central Black Range, New Mexico, in the regional geologic framework of south-central New Mexico [Ph.D. dissertation]: Socorro, New Mexico Institute of Mining and Technology, 402 p.

Hawley, J.W., comp., 1978, Guidebook to Rio Grande rift in New Mexico and Colorado: New Mexico Bureau of Mines and Mineral Resources, Circular 163, 241 p.

Hawley, J.W., and Haase, C.S., comps., 1992, Hydrogeologic framework of the northern Albuquerque Basin: New Mexico Bureau of Mines and Mineral Resources, Open-file Report 387, 165 p., 7 plates.

Hawley, J.W., and Whitworth, T.M., comps., 1996, Hydrogeology of potential recharge areas for the basin- and valley-fill aquifer systems, and hydrogeochemical modelling of proposed artificial recharge of the upper Santa Fe aquifer, northern Albuquerque Basin, New Mexico: New Mexico Bureau of Mines and Mineral Resources, Open-file Report 402-D, 575 p.

Hawley, J.W., Kottlowski, F.E., Strain, W.S., Seager, W.R., King, W.E., and LeMone, D.V., 1969, The Santa Fe Group in the south-central New Mexico border region, *in* Kottlowski, F.E., and LeMone, D.V., eds., Border Stratigraphy Symposium: New Mexico Bureau of Mines and Mineral Resources, Circular 104, 52–76 p.

Hawley, J.W., Kennedy, J.F., Granados-Olivas, A., and Ortiz, M.A., 2009, Hydrogeologic framework of the

binational western Hueco bolson-Paso del Norte area, Texas, New Mexico, and Chihuahua: overview and progress report on digital-model development: New Mexico Water Resources Research Institute, Technical Completion Report 349, 45 p.

Hermann, M.L., 1986, Geology of the southwestern San Mateo Mountains, Socorro County, New Mexico [M.S. thesis]: Socorro, New Mexico Institute of Mining and Technology, 192 p.

Ingram, R.L., 1954, Terminology for the thickness of stratification and parting units in sedimentary rocks: Geological Society of America Bulletin, v. 65, p. 937–938.

Jochems, A.P., 2015, Geologic map of the Williamsburg NW 7.5-minute quadrangle, Sierra County, New Mexico: New Mexico Bureau of Geology and Mineral Resources, Open-File Geologic Map OF-GM 251, scale 1:24,000 (revised 2019).

Jochems, A.P., and Cox, B.E., 2019, Geologic map of the Priest Tank 7.5-minute quadrangle, Sierra County, New Mexico: New Mexico Bureau of Geology and Mineral Resources, Open-File Geologic Map OF-GM 275, scale 1:24,000.

Jochems, A.P., and Koning, D.J., 2015a, Geologic map of the Williamsburg 7.5-minute quadrangle, Sierra County, New Mexico: New Mexico Bureau of Geology and Mineral Resources, Open-File Geologic Map OF-GM 250, scale 1:24,000 (revised 2019).

Jochems, A.P., and Koning, D.J., 2015b, Holocene stratigraphy and a preliminary geomorphic history for the Palomas basin, south-central New Mexico: New Mexico Geology, v. 37, p. 77–88.

Jochems, A.P., and Koning, D.J., 2017, Geologic map of the Clark Spring Canyon 7.5-minute quadrangle, Sierra County, New Mexico: New Mexico Bureau of Geology and Mineral Resources, Open-File Geologic Map OF-GM 263, scale 1:24,000.

Keller, G.R., 1983, Bouguer gravity anomaly map of the Socorro region, *in* Chapin, C.E. and Callender, J.F., eds., Socorro Region II: New Mexico Geological Society, Guidebook 34, p. 96.

Kelley, V.C., 1952, Tectonics of the Rio Grande depression of central New Mexico, *in* Johnson, R.B. and Read, C.B., eds., Rio Grande County: New Mexico Geological Society, Guidebook 6, p. 92–105.

Kelley, V.C., 1977, Geology of Albuquerque Basin, New Mexico: New Mexico Bureau of Mines and Mineral Resources, Memoir 33, 60 p.

Koning, D.J., Connell, S.D., Pazzaglia, F.J., and McIntosh, W.C., 2002, Redefinition of the Ancha Formation and Pliocene-Pleistocene deposition in the Santa Fe embayment, north-central New Mexico: New Mexico Geology, v. 24, p. 75–87.

Koning, D.J., Jochems, A.P., Kelley, S.A., McLemore, V.T., and Cikoski, C.T., 2014, Geologic map of the Monticello 7.5-minute quadrangle, Sierra and Socorro Counties, New Mexico: New Mexico Bureau of Geology and Mineral Resources, Open-File Geologic Map OF-GM 245, scale 1:24,000.

Koning, D.J., Jochems, A.P., and Cikoski, C.T., 2015, Geologic map of the Skute Stone Arroyo 7.5-minute quadrangle, Sierra County, New Mexico: New Mexico Bureau of Geology and Mineral Resources, Open-File Geologic Map OF-GM 252, scale 1:24,000.

Koning, D.J., Jochems, A.P., Morgan, G.S., Lueth, V., and Peters, L., 2016, Stratigraphy, gravel provenance, and age of early Rio Grande deposits exposed 1-2 km northwest of downtown Truth or Consequences, New Mexico, *in* Frey, B.A., Karlstrom, K.E., Lucas, S.G., Williams, S., Zeigler, K., McLemore, V., and Ulmer-Scholle, D.S., eds., The Geology of the Belen Area: New Mexico Geological Society, Guidebook 67, p. 459–478.

Koning, D.J., Jochems, A.P., and Heizler, M.T., 2018, Early Pliocene paleovalley incision during early Rio Grande evolution in southern New Mexico, *in* Mack, G.H., Hampton, B.A., Ramos, F.C., Witcher, J.C., and Ulmer-Scholle, D.S., eds., Las Cruces Country III: New Mexico Geological Society, Guidebook 69, p. 93–108.

Kottlowski, F.E., 1960, Summary of Pennsylvanian sections in southwestern New Mexico and southeastern Arizona: New Mexico Bureau of Mines and Mineral Resources, Bulletin 66, 187 p.

Kucks, R.P., Hill, P.L., and Heywood, C.E., 2001, New Mexico aeromagnetic and gravity maps and data: a web site for distribution of data: U.S. Geological

Survey Open-File Report 01-0061, http://pubs.usgs.gov/of/2001/ofr-01-0061/html/newmex.htm.

Kuiper, K.F., Deino, A., Hilgen, F.J., Krijgsman, W., Renne, P.R., and Wijbrans, J.R., 2008, Synchronizing rock clocks of Earth history: Science, v. 320, p. 500–504, doi:10.1126/science.1154339.

Land, L., 2016, Overview of fresh and brackish water quality in New Mexico: New Mexico Bureau of Mines and Mineral Resources, Open-file Report 583, 55 p.

Lozinsky, R.P., 1986, Geology and late Cenozoic history of the Elephant Butte area, Sierra County, New Mexico: New Mexico Bureau of Mines and Mineral Resources, Circular 187, 40 p.

Lozinsky, R.P., and Hawley, J.W., 1986a, The Palomas Formation of south-central New Mexico—a formal definition: New Mexico Geology, v. 8, p. 73–78, 82.

Lozinsky, R.P., and Hawley, J.W., 1986b, Upper Cenozoic Palomas Formation of south-central New Mexico, *in* Clemons, R.E., King, W.E., Mack, G.H., and Zidek, J., eds., Truth or Consequences Region: New Mexico Geological Society, Guidebook 37, p. 239–247.

Lucas, S.G., Krainer, K., and Spielmann, J.A., 2012, Pennsylvanian stratigraphy in the Fra Cristobal and Caballo Mountains, Sierra County, New Mexico, *in* Lucas, S.G., McLemore, V.T., Lueth, V.W., Spielmann, J.A., and Krainer, K., eds., Geology of the Warm Springs Region: New Mexico Geological Society, Guidebook 63, p. 327–344.

Lucas, S.G., Krainer, K., Barrick, J.E., and Vachard, D., 2016, The Pennsylvanian System in the Mud Springs Mountains, Sierra County, New Mexico, USA: New Mexico Museum of Natural History and Science, Bulletin 69, p. 1–58.

Lucas, S.G., Krainer, K., Allen, B.D., and Barrick, J.E., 2017, The Paleozoic section at Bell Hill, Socorro County, New Mexico: New Mexico Museum of Natural History and Science, Bulletin 77, p. 263–286.

Lynch, S.D., 2003, Geologic mapping and 40Ar/39Ar geochronology in the northern Nogal Canyon caldera, within and adjacent to the southwest corner of the Blue Mountain quadrangle, San Mateo Mountains, New Mexico [M.S. thesis]: Socorro, New Mexico Institute of Mining and Technology, 102 p., 1 plate, 1:24,000.

Machette, M.N., and Jochems, A.P., comps., 2016a, Fault number 2130, Black Hill fault, in Quaternary fault and fold database of the United States: https://earthquakes.usgs.gov/hazards/qfaults (accessed June 2019).

Machette, M.N., and Jochems, A.P., comps., 2016b, Fault number 2016, Milligan Gulch fault zone, in Quaternary fault and fold database of the United States: https://earthquakes.usgs.gov/hazards/qfaults (accessed June 2019).

Mack, G.H., Salyards, S.L., and James, W.C., 1993, Magnetostratigraphy of the Plio-Pleistocene Camp Rice and Palomas Formations in the Rio Grande rift of southern New Mexico: American Journal of Science, v. 293, p. 49–77.

Mack, G.H., Seager, W.R., and Kieling, J., 1994, Late Oligocene and Miocene faulting and sedimentation, and evolution of the southern Rio Grande rift, New Mexico, USA: Sedimentary Geology, v. 92, p. 79–96.

Mack, G.H., Salyards, S.L., McIntosh, W.C., and Leeder, M.R., 1998, Reversal magnetostratigraphy and radioisotopic geochronology of the Plio-Pleistocene Camp Rice and Palomas Formations, southern Rio Grande rift, *in* Mack, G.H., Austin, G.S., and Barker, J.M., eds., Las Cruces Country II: New Mexico Geological Society, Guidebook 49, p. 229–236.

Mack, G.H., Cole, D.R., and Treviño, L., 2000, The distribution and discrimination of shallow, authigenic carbonate in the Pliocene-Pleistocene Palomas Basin, southern Rio Grande rift: Geological Society of America Bulletin, v. 112, p. 643–656.

Mack, G.H., Seager, W.R., Leeder, M.R., Perez-Arlucea, M., and Salyards, S.L., 2006, Pliocene and Quaternary history of the Rio Grande, the axial river of the southern Rio Grande rift, New Mexico, USA: Earth-Science Reviews, v. 79, p. 141–162.

Maxwell, C.H., and Oakman, M.R., 1990, Geologic map of the Cuchillo quadrangle, Sierra County, New Mexico: U.S. Geological Survey, Geologic Quadrangle Map GQ-1686, scale 1:24,000.

McCraw, D.J., and Love, D.W., 2012, An overview and delineation of the Cuchillo geomorphic surface, Engle and Palomas Basins, New Mexico, *in* Lucas, S.G., McLemore, V.T., Lueth, V.W., Spielmann,

and early Pleistocene) faunas from New Mexico: Bulletin of the American Museum of Natural History, v. 279, p. 269–320.

Morgan, G.S., and Lucas, S.G., 2012, Cenozoic vertebrates from Sierra County, southwestern New Mexico, *in* Lucas, S.G., McLemore, V.T., Lueth, V.W., Spielmann, J.A., and Krainer, K., eds., Geology of the Warm Springs Region, New Mexico Geological Society, Guidebook 63, p. 525–540.

Munsell Color, 2009, Munsell soil color book: Grand Rapids, MI, X-Rite.

Nelson, E.P., 1986, Geology of the Fra Cristobal Range, south-central New Mexico, *in* Clemons, R.E., King, W.E., Mack, G.H., and Zidek, J., eds., Truth or Consequences Region: New Mexico Geological Society, Guidebook 37, p. 83–95.

Nelson, W.J., Lucas, S.G., Krainer, K., and Elrick, S., 2013, The Gray Mesa Formation (Middle Pennsylvanian) in New Mexico: New Mexico Museum of Natural History and Science, Bulletin 59, p. 101–122.

Osburn, G.R., 1984, Socorro County geologic map: New Mexico Bureau of Mines and Mineral Resources, Open-file Report 238, scale 1:200,000.

Osburn, G.R., and Chapin, C.E., 1983, Ash-flow tuffs and cauldrons in the northeast Mogollon-Datil volcanic field: a summary, *in* Chapin, C.E. and Callender, J.F., eds., Socorro Region II: New Mexico Geological Society, Guidebook 34, p. 197–204.

Repenning, C.A., and May, S.R., 1986, New evidence for the age of lower part of the Palomas Formation, *in* Clemons, R.E., King, W.E., Mack, G.H., and Zidek, J., eds., Truth or Consequences Region: New Mexico Geological Society, Guidebook 37, p. 257–260.

Seager, W.R., Hawley, J.W., and Clemons, R.E., 1971, Geology of San Diego Mountain area, Doña Ana County, New Mexico: New Mexico Bureau of Mines and Mineral Resources, Bulletin 97, 38 p.

Seager, W.R., Shafiqullah, M., Hawley, J.W., and Marvin, R.F., 1984, New K-Ar dates from basalts and the evolution of the southern Rio Grande rift: Geological Society of America Bulletin, v. 95, p. 87–99.

Soil Survey Staff, 1999, Soil taxonomy: U.S. Department of Agriculture, US. Department of Agriculture Handbook 436, 869 p.

Udden, J.A., 1914, Mechanical composition of clastic sediments: Geological Society of America Bulletin, v. 25, p. 655–744.

USDA, 2008, Natural Agricultural Imagery Program (NAIP) factsheet: U.S. Department of Agriculture, 2 p.

Weissmann, G.S., Hartley, A.J., Nichols, G.J., Scuderi, L.A., Olson, M., Buehler, H., and Banteah, R., 2010, Fluvial form in modern continental sedimentary basins: distributive fluvial systems: Geology, v. 38, p. 39–42, doi:10.1130/G30242.1.

Wentworth, C.K., 1922, A scale of grade and class terms for clastic sediments: Journal of Geology, v. 30, p. 377–392.

Western Regional Climate Center, 2019, Bosque del Apache, New Mexico NCDC 1981-2010 monthly normals: https://wrcc.dri.edu/cgi-bin/cliMAIN.pl?nm1138 (accessed June 2019).

Western Regional Climate Center, 2019, Rienhardt Ranch, New Mexico NCDC 1981-2010 monthly normals: https://wrcc.dri.edu/cgi-bin/cliMAIN.pl?nm7423 (accessed June 2019).

White, J.D.L., and Houghton, B.F., 2006, Primary volcaniclastic rocks: Geology, v. 34, p. 677–680.

Winter, J.D., 2010, Principles of igneous and metamorphic petrology: Upper Saddle River, NJ, Pearson/Prentice Hall, 702 p.

APPENDIX A

Detailed descriptions of lithologic units on the
Black Hill 7.5-minute quadrangle

QUATERNARY

Anthropogenic and Eolian Units

af Anthropogenic Fill (Modern to ~50 years old) – Thick accumulations of sand, gravel, and clayey-silty sand from construction activities. Mapped for thick road fill along Interstate 25 and New Mexico Highway 1 as well as dams impounding stock tanks. Thickness is 1–10 m.

ae Anthropogenic Excavated Ground (Modern to ~50 years old) – Excavations associated with stock tank impoundments and quarries.

afe Anthropogenic Fill and Excavated Ground, undivided (Modern to ~50 years old) – Gravelly sand fill (af) and excavations (ae). See descriptions of each unit.

Qes Eolian sand and sheetwash, undivided (Holocene) – Loose sand underlying sheets, coppice dunes, and small blowouts (<0.75 m deep). Sand is grayish-brown to brown (10YR 5/2-3), non-calcareous, massive to low-angle planar cross-stratified or laminated, moderately to moderately well-sorted, subrounded to well-rounded, and very fine- to medium-grained. Grains are composed of 75–80% quartz, 10–15% lithics (volcanic and ferromagnesian minerals), and 10–15% feldspar with no clay. Occasional to common (15–30%), fine to very coarse pebbles at surface are weathered from underlying basin-fill units. Soil development is weak to non-existent. Generally less than 2–2.5 m thick.

Valley-Floor Units

Qam Modern Alluvium (Modern to ~50 years old) – Loose gravelly sand and gravel forming bars and underlying channels in ephemeral drainages. Sand consists of brown to grayish-brown (7.5YR 5/4 to 10YR 5/2), very poorly to poorly sorted, angular to rounded (mostly subangular), fU-vcU grains (up to 10% vfL-fL) composed of 85–90% lithics (felsic volcanic), 5–10% feldspar, and up to 5% quartz with no clay. Gravel consist of clast-supported, subangular to rounded (mostly subangular to subrounded), poorly to moderately sorted pebbles, cobbles, and subordinate boulders (up to 15–20% where stream courses run adjacent to uplands). Clast lithologies are mostly fine-grained, felsic volcanic clasts. Longitudinal and transverse bars are often underlain by up to 80% very poorly sorted, subrounded to rounded, well-graded pebbles through coarse cobbles. No topsoil present. Bar-and-swale topography and occasional steep-walled channels characterize the surface, exhibiting up to 0.1–0.3 m of relief. Thickness is 1–4(?) m.

Qamh Modern and Historical Alluvium, undivided (Upper Holocene) – Modern alluvium (Qam) and subordinate historical alluvium (Qah). See detailed descriptions of each unit.

Qamy Modern and Younger Alluvium, undivided (Holocene) – Modern alluvium (Qam) and subordinate younger alluvium (Qay). See detailed descriptions of each unit.

Qar Recent (Historical + Modern) Alluvium (Upper Holocene) – Historical alluvium (Qah) and modern alluvium (Qam) in approximately equal proportions. See detailed descriptions of each unit.

Qary Recent (Historical + Modern) and Younger Alluvium, undivided (Holocene) – Recent alluvium (Qah + Qam) and subordinate younger alluvium (Qay). See detailed descriptions of each unit.

Qah Historical Alluvium (Upper Holocene) – Loose to very weakly consolidated, gravelly sand and sandy gravel underlying low terraces along valley floors in thin to thick (3–30+ cm), mostly lenticular (occasionally tabular) beds. Sand may be pebbly and massive to horizontal-planar laminated or, less commonly, cross-laminated. Sand is brown to yellowish-brown (7.5YR 4/4 to 10YR 5/3-4), moderately to strongly calcareous, very poorly to poorly sorted, subangular to subrounded, fine- to very coarse-grained (<7% very fine sand and silt-clay), and a volcanic litharenite. Trace to 3% brownish clay films are observed in matrix. Gravel consist of clast-supported, imbricated, poorly sorted, subangular to well-rounded pebbles and subordinate cobbles of felsic volcanics, particularly Vicks Peak Tuff. Deposit may feature 5–10% lenses of massive to vaguely low-angle cross-stratified sand similar to gravel matrix. Weak topsoil development characterized

by fine peds that have experienced no or very minor clay illuviation (as bridges) and stage I carbonate accumulation. The surface exhibits bar-and-swale topography and is locally eroded, with up to 0.2 m of surface relief and no clast varnishing. Tread height is 0.3–1.5 m above modern grade. Thickness is 0.1–2.0 m.

Qahm Historical and Modern Alluvium, undivided (Upper Holocene) – Historical alluvium (Qah) and subordinate modern alluvium (Qam). See detailed descriptions of each unit.

Qahy Historical and Younger Alluvium, undivided (Holocene) – Historical alluvium (Qah) and subordinate younger alluvium (Qay). See detailed descriptions of each unit.

Qay Younger Alluvium (Holocene) – Weakly consolidated gravelly sand and sandy gravel underlying low terraces adjoining active channels or relatively inactive valley floors. Locally fines upward. Gravel are subangular to subrounded and composed of fine-grained, felsic volcanic rocks, particularly Vicks Peak Tuff, with 1–5% feldspar porphyries. Sand is reddish-brown to brown or strong brown (5YR 4/4; 7.5YR 4-5/4-6; 7.5-10YR 5/3), subangular, and very fine- to very coarse-grained with 1–10% clay-silt. Sandy gravel is clast-supported in very thin to medium, tabular to lenticular beds. Gravel consist of weakly to moderately imbricated, poorly sorted, subangular (mostly) to subrounded pebbles with 10–30% cobbles and trace to 5% boulders. Clast lithologies include fine-grained tuff and rhyolite with 1–5% feldspar porphyries. Gravel matrix consists of brown to strong brown (7.5YR 4-5/4-6; 7.5-10YR 5/3), poorly sorted, angular to subrounded (mostly subangular), very fine- to very coarse-grained sand with 1–5% silt-clay; sand is composed chiefly of lithic (volcanic) grains. Topsoil and buried soils are characterized by brown to strong brown (7.5YR 4-5/4-6), illuviated clay (Bt) horizons (faint to distinct clay films on ped faces or clast surfaces) exhibiting weak to moderate, fine to coarse, angular to subangular blocky peds. These clayey horizons may have weak calcium carbonate precipitation or overlie calcic horizons (stage I to II carbonate accumulation). Locally, deposit lacks Bt horizon and is instead characterized by a darkened A horizon with ped development. Elsewhere, soils have been removed entirely by surface erosion. Geomorphic surfaces lack bar-and-swale topography. Tread height is 1–2.2 m above modern grade. Thickness is 1–5(?) m.

Qaym Younger and Modern Alluvium, undivided (Holocene) – Younger alluvium (Qay) and subordinate modern alluvium (Qam). See detailed descriptions of each unit.

Qayh Younger and Historical Alluvium, undivided (Holocene) – Younger alluvium (Qay) and subordinate historical alluvium (Qah). See detailed descriptions of each unit.

Qayr Younger and Recent (Historical + Modern) Alluvium, undivided (Holocene) – Younger alluvium (Qay) and subordinate recent alluvium (Qah + Qam). See detailed descriptions of each unit.

Qayrt Younger and Recent (Historical + Modern) Alluvium, Transitional Deposits (Holocene) – Younger alluvium (Qay) and subordinate recent alluvium (Qah + Qam) in non-dissected, low order drainages. Poorly exposed. See detailed descriptions of each unit.

Terrace Units

Qtu Terrace gravels in smaller drainages, undivided (Upper to Middle Pleistocene) – Loose to moderately consolidated, sandy gravel, and gravelly sand in very thin to thick (1–80 cm), tabular to lenticular beds underlying terraces along higher order stream courses. Gravel are clast-supported and well-imbricated to locally trough or planar cross-stratified (foresets 20–40 cm thick). Clasts consist of very poorly to poorly sorted, subangular to well-rounded pebbles, cobbles (10–60%), and boulders (1–25%). Clast lithologies are mostly or entirely fine-grained felsic volcanics with trace to a few percent each of feldspar porphyry, chert, and/or intermediate volcanics (visual estimate). Gravel matrix consists of yellowish-red to strong brown (5YR 4-5/6; 7.5YR 5/6) to light- or pale brown (7.5YR 6/3-4; 10YR 6/3), non- or weakly to strongly calcareous, very poorly to moderately sorted, subangular to rounded, vfU-vcL sand (mostly mL-vcL) composed of 80–90% lithics (volcanic) and 10–20% quartz+feldspar with 0–10% reddish-brown clay bridges and films. Compared to unit Qppu, gravel are browner, less consolidated, less commonly cross-stratified, and coarser. Gravel may be intercalated with minor lenses of thin, tabular beds of silty, very fine- to fine-grained sand or pebbly sand (very fine to very coarse) that are horizontal-planar or cross-laminated to trough cross-stratified. Soils and surface characteristics generally vary with age; moderate to

strong calcic horizons (stage II-IV carbonate accumulation), illuviated clay (Bt, Btk horizons where not eroded), and various degrees of desert pavement development and clast varnishing may be observed at the surface. Deposit lacks bar-and-swale topography and buried soils. Terrace treads diverge in a downstream direction and are not necessarily correlative between drainages. Thickness is 0.3–9 m. Subdivided into four allostratigraphic subunits distinguished by tread height above valley floors:

Qtl Lower Terrace Gravel (Upper Pleistocene) – Sandy gravel with 15–40% cobbles and 1–10% boulders. Commonly features illuviated clay (Bt) horizon in topsoil. Weak varnish on 20–30% of surface clasts. Tread generally lies 1.5–3 m above valley floors. Deposit is 0.3–1 m thick.

Qtm Middle Terrace Gravel (Upper Pleistocene) – Sandy gravel in very thin to medium, mostly lenticular beds (minor tabular beds); thick beds and cross-stratification (up to 0.4 m thick) locally present. Deposit contains 1–10% sand or silty sand beds. Gravel is weakly to moderately consolidated, clast-supported, imbricated, subrounded, poorly sorted (locally moderately sorted within a particular bed), and comprised of pebbles with 25–50% cobbles and 2–3% boulders. Gravel are composed primarily of fine-grained felsites with <5% feldspar porphyry, 0–5% black-speckled and quartz-phyric felsite (absent south of Crawford Hollow), and 1–5% coarser-grained felsites (>3% visible quartz and feldspar crystals). Gravel matrix consists of light-brown to reddish-yellow (7.5-10YR 6/3 to 7.5YR 6/4-6), subangular to subrounded, poorly sorted, medium- to very coarse-grained sand (<25% very fine to fine sand) dominated by lithic (volcanic) grains with 1–5% free clay. Topsoil is characterized by Bt horizon development in upper 60 cm (distinct clay films on half to most of clast surface). Highly scoured base. In Sheep Canyon west of Interstate 25, this terrace deposit correlates upstream with Qpw1. Tread lies 2–4 m above the modern drainage. Thickness is 0.5–2.7 m.

Qth Higher Terrace Gravel (Upper? to Middle Pleistocene) – Variable preservation of surface soil. Weak desert pavement and moderately strong varnish on 45–60% of surface clasts. Tread generally lies at least 4–6 m above valley floors and 1–3 m above Qtm tread.

Qtvh Highest Terrace Gravel (Middle Pleistocene) – Strongest soil development observed is stage III(+) to IV calcic soil horizons 10–100 cm thick. Weakly to well-developed desert pavement. Moderate varnish on 20–65% of surface clasts. Tread lies 7–16 m above valley floors, decreasing to 3–5 m at up-drainage positions.

Qtc Terrace Gravels of Crawford Hollow, undivided (Upper to Middle Pleistocene) – Moderately consolidated, sandy gravel in vague, thin to thick, tabular to (mostly) lenticular beds. Very weakly clay-cemented. Gravel consists of clast-supported, imbricated, poorly sorted, subangular to subrounded pebbles with subordinate cobbles and boulders (more abundant near the base). Clast lithologies include fine-grained felsites with 1–3% feldspar porphyry, 0–5% intermediate volcanics, and up to 1% black-speckled and quartz-phyric felsite observed in Qtu gravels in the northern part of the quadrangle. The matrix consists of yellowish-red to brown or strong brown (5-7.5YR 4-5/6), poorly sorted, subangular to subrounded, fine- to very coarse-grained (mostly mL-vcU) sand dominated by lithics (volcanic) and with 1–5% clay. Where not eroded, the topsoil exhibits an illuviated clay (Bt or Btk) horizon underlain by a moderate to strong calcic horizon (stage II to III carbonate accumulation). Compared to the underlying Palomas Formation, terrace deposits are browner, more poorly sorted, and slightly less consolidated. Terrace treads diverge in a downstream direction, becoming higher above the floor of Crawford Hollow. Thickness is 0.3–10 m. Subdivided into four to six allostratigraphic subunits:

Qtc1 Lower terrace Gravel of Crawford Hollow (Upper Pleistocene) – Tread lies 2–7 m above the valley floor, decreasing upstream. May locally be subdivided into two subunits (not mapped) whose treads differ about 1 m in height. It is not known if these represent separate depositional events or if the lower is a fill-cut terrace. Deposit is 0.3–1 m thick.

Qtc2 Lower-Middle Terrace Gravel of Crawford Hollow (Upper to Middle Pleistocene) – Tread lies 3–8 m above the valley floor, decreasing upstream.

Qtc3 Middle Terrace Gravel of Crawford Hollow (Middle Pleistocene) – In general, terrace level lies 6–9 m above the valley floor, but typically 2–4 terrace treads lie in close proximity. These treads are likely developed on the same fill and locally may lie on the same fill as Qtc4. Locally subdivided into two subunits (not mapped) whose treads differ by about 1–3 m in height.

Qtc4 Upper-Middle Terrace Gravel of Crawford Hollow (Middle Pleistocene) – Sandy gravel and lesser pebbly sand that forms a notably thick fill deposit in much of the canyon. Sandy gravel is in thin to thick, lenticular to tabular beds. Gravel is clast-supported, commonly imbricated, subrounded, very poorly to poorly sorted, and comprised of very fine to very coarse pebbles with 20–40% cobbles and 5–15% boulders. Basal beds often have approximately subequal proportions of pebbles and cobbles. Clast lithologies include fine-grained felsites with 1% feldspar porphyry, 3–5% other intermediate volcanic clasts, 1–5% coarser-grained felsites (>3% visible crystals of quartz and feldspar), and trace to 2% black-speckled and quartz-phyric felsite. Pebbly sand is very thin to laminated and horizontal-planar. Sand is typically strong brown to reddish-yellow (7.5YR 4-6/6), subangular to (mostly) subrounded, poorly sorted, medium to very coarse grained (less than 20% very fine to fine sand), and dominated by volcanic grains with 1–5% free clay (very locally up to 15% clay and reddish-brown color). Moderately consolidated and very weakly to weakly clay-cemented. Top soil has a Bt horizon that is 50–60 cm thick and underlain by a stage III to III+ calcic horizon. Lower contact is scoured. Tread lies about 10–16 m above the valley floor, decreasing to ~4 m near the western quadrangle boundary. Two subunits, Qtc4a and Qtc4b, can be differentiated that differ 1–2 m in geomorphic height. In the central part of the canyon, the tread lies ~2 m below the next higher geomorphic surface. Thickness is 1-10 m.

Qtc5 Upper Terrace Gravel of Crawford Hollow (Middle Pleistocene) – A rare gravelly deposit with a tread that lies 1–3 m above Qtc4b east of Interstate 25. Other surfaces in a similar geomorphic position are erosional. Thickness is <2-4 m.

Qtn Terrace Gravels of Nogal Canyon, undivided (Upper to Middle Pleistocene) – Loose to moderately consolidated sandy gravel and sand in thin to thick (45–120 cm), tabular to broadly lenticular beds underlying terraces along Nogal Canyon. Gravel are clast-supported and well-imbricated to trough cross-stratified. Clasts consist of very poorly to poorly sorted, subrounded to well-rounded pebbles (55–95%), cobbles (5–45%), and boulders (usually <5%). Clast lithologies are mostly or entirely felsic volcanics with trace to a few percent each of feldspar porphyry and/or intermediate volcanics (visual estimate). Gravel matrix consists of reddish-brown (5YR 5/3-4) to strong brown (7.5YR 5/6), poorly sorted, subrounded to rounded, vfL-cL sand composed of 85–90% lithics (volcanic) and 10–15% quartz+feldspar with 10–20% reddish to brownish clay bridges and films. Gravel may be intercalated with rare lenses of sand similar to gravel matrix. Underlying strata may be scoured up to 0.6 m. Soils and surface characteristics generally vary with age; moderate to strong calcic horizons (stage II-III carbonate accumulation), illuviated clay horizons (where not eroded), and various degrees of desert pavement development and clast varnishing may be observed at the surface. Deposit lacks bar-and-swale topography. Terrace treads diverge in a downstream direction. Thickness is 1.5–4 m. Subdivided into five to six allostratigraphic subunits distinguished by tread height above the canyon floor:

Qtn1 Lower Terrace Gravel of Nogal Canyon (Upper Pleistocene) – Near the southeastern corner of the quadrangle, two subunits, Qtn1a and Qtn1b, can be differentiated by a ~2-m-tall riser. Tread lies 7–9 m above valley floors.

Qtn2 Lower-Middle Terrace Gravel of Nogal Canyon (Upper Pleistocene) – Tread lies 27–30 m above valley floors.

Qtn3 Middle Terrace Gravel of Nogal Canyon (Upper? to Middle Pleistocene) – Tread lies 42–48 m above valley floors.

Qtn4 Upper-Middle Terrace Gravel of Nogal Canyon (Middle Pleistocene) – Strongest soil development observed is stage III(+) calcic soil in upper 1.3 m of deposit. Weakly to well-developed desert pavement. Weak to moderate varnish on 25–45% of surface clasts. Tread lies 51–58 m above valley floors.

Qtn5 Upper Terrace Gravel of Nogal Canyon (Middle Pleistocene) – Strongest soil development observed is stage IV calcic soil in upper 1 m of deposit. Moderately to well-developed desert pavement. Weak to strong varnish on 15–60% of surface clasts. Tread lies 65–73 m above valley floors.

Qts4 Upper Terrace Gravel of Silver Canyon (Middle Pleistocene) – Loose to weakly consolidated sandy gravel and silt-sand in thick (50–80 cm), tabular to broadly lenticular beds underlying terraces along Silver Canyon. Gravel are clast-supported and moderately well-imbricated. Clasts consist of poorly sorted, subrounded to

rounded pebbles (50–100%) and cobbles (0–50%) dominated by felsic volcanics. Gravel matrix consists of brown (7.5YR 4-6/4), strongly calcareous, very poorly to poorly sorted, subrounded to rounded, vfU-cU sand composed of 80–85% lithics (volcanic) and 15–20% quartz+feldspar with <5% brownish chips. Deposit features up to 10–15% lenses of strong brown (e.g., 7.5YR 5/6), mostly tabular, internally massive to low-angle cross-stratified or laminated, slightly pebbly silt to fL or mU sand. Strongest soil development observed is stage IV calcic soil in upper 30 cm of deposit. Moderate desert pavement development and weak to strong varnish on 10–50% of surface clasts observed. Tread lies 3–18 m above valley floors. Thickness is 1.9–12 m.

Alluvial Fan and Piedmont Units

Qfm Modern Fan Alluvium (Modern to ~50 years old) – Loose gravelly sand and sandy gravel underlying fan channels, bars, and levees. Sand consists of brown to yellowish-brown (10YR 5/3-4), non- to very weakly calcareous, very poorly to poorly sorted, angular to rounded, fL-cU grains composed of 55–60% quartz, 30–35% lithics (volcanic), and 10–15% feldspar with no clay. Gravel include sandy pebble-cobble and pebble-cobble-boulder deposits; clast proportions include 55–90% pebbles, 10–45% cobbles, and 0–10% small boulders of mostly felsic lithologies reworked from Palomas Formation basin fill and terrace gravels. Soils are not observed. Bar-and-swale topography characterizes the surface, exhibiting up to 0.4–0.5 m of relief. Thickness is <2–3 m in most places.

Qfmh Modern and Historical Fan Alluvium, undivided (Upper Holocene) – Modern (Qfm) and subordinate historical fan alluvium (Qfh). See detailed descriptions of each unit.

Qfh Historical Fan Alluvium (Upper Holocene) – Loose pebble-cobble gravel in medium to thick (20–40+ cm), tabular to vaguely wedge-shaped beds. Gravel are clast- to matrix-supported and internally massive to crudely imbricated. Clasts consist of poorly sorted, angular to subrounded pebbles (65–95%) and cobbles (5–35%) of felsic lithologies; up to 15–20% of clasts may represent exotic lithologies (e.g., quartzite) derived from the axial-fluvial facies of the Palomas Formation. Gravel matrix consists of dark-brown to brown (7.5YR 3-4/4), very weakly calcareous, very poorly sorted, angular to rounded, fU-vcL sand composed of 45–50% lithic (volcanic), 40–45% quartz, and 5–15% feldspar with <5–7% light brownish clay films. Soils are not observed; moderate to strong bioturbation by very fine to coarse roots. No clast varnish observed at surface. Bar-and-swale topographic relief is up to 0.25–0.4 m. Thickness is <2–3 m in most places.

Qfr Recent (Historical + Modern) Fan Alluvium (Upper Holocene) – Historical (Qfh) and modern fan alluvium (Qfm) in approximately equal proportions. See detailed descriptions of each unit.

Qfry Recent (Historical + Modern) and Younger Fan Alluvium, undivided (Holocene) – Recent (Qfh + Qfm) and subordinate younger fan alluvium (Qfy). See detailed descriptions of each unit.

Qfy Younger Fan Alluvium (Holocene) – Loose pebble-cobble gravel in medium to thick (25–80 cm), tabular to wedge-shaped beds. Gravel are mostly clast-supported and internally massive to crudely imbricated. Clasts consist of very poorly to poorly sorted, subangular to rounded pebbles (60–90%) and cobbles (10–40%) of >95% felsic volcanic lithologies. Gravel matrix consists of brown (7.5YR 4/2-4 or 5/4), moderately to strongly calcareous, very poorly sorted, subangular to rounded, silty, fL-cU sand composed of 70–80% lithic (volcanic), 15–20% quartz, and 10–15% feldspar grains with up to 10% brownish clay films. Stage I calcic horizon with illuviated clay (Btk) observed in upper 25 cm. Weak varnish on no more than 10% of surface clasts. Bar-and-swale topographic relief up to 15–20 cm. Tread height 1.7–2.2 m above modern grade (minimum thickness).

Qfym Younger and Modern Fan Alluvium, undivided (Holocene) – Younger (Qfy) and subordinate modern fan alluvium (Qfm). See detailed descriptions of each unit.

Qfyh Younger and Historical Fan Alluvium, undivided (Holocene) – Younger (Qfy) and subordinate historical fan alluvium (Qfh). See detailed descriptions of each unit.

Qfyr Younger and Recent (Historical + Modern) Fan Alluvium, undivided (Holocene) – Younger (Qfy) and subordinate recent fan alluvium (Qfh + Qfm). See detailed descriptions of each unit.

Qfo Older fan alluvium (Lower Holocene to Upper Pleistocene) – Loose pebble and pebble-cobble gravel in thick to very thick (75–160 cm), tabular to wedge-shaped beds. Gravel are clast- to occasionally matrix-supported and internally massive to moderately imbricated. Clasts consists of very poorly to poorly sorted, subangular to rounded pebbles (55–95%), cobbles (5–45%), and boulders (0–5%) of >95% felsic volcanic lithologies. Gravel matrix consists of brown to strong brown (7.5YR 4/4-6), moderately calcareous, poorly to moderately sorted, angular to rounded, fU-cU sand composed of 50–55% lithic (volcanic and ferromagnesian minerals), 35–40% quartz, and 5–15% feldspar grains with no clay. Stage I calcic horizon observed in upper 40 cm. Weak varnish on 25–40% of surface clasts. Tread height 2.1–3.2 m above modern grade (minimum thickness).

Qpw1 Lower western pediment deposit (Lower Holocene to Upper Pleistocene) – Silt, sand, and subangular to rounded pebble-cobble and pebble-cobble-boulder gravels filling shallowly incised valleys in the north-central part of the quadrangle. Clast lithologies are felsic volcanics derived from the east-central San Mateo Mountains. Surface features an overall grayish color. Thickness is <2–3 m.

QUATERNARY-TERTIARY

Basin-fill Units

Qppu Upper Piedmont Facies of the Palomas Formation (Lower Pleistocene) – Interbedded gravel bodies, pebbly silt-sand, silt, and mud. Unit consists of >80% gravels where it underlies proximal to medial positions of a Nogal Canyon paleofan extending from the southern quadrangle boundary north to Crawford Hollow. This proportion drops to 20–50% in the northern and eastern parts of the quadrangle (east of Interstate 25). Gravels occur in medium to very thick (20–110+ cm; minor very thin to thin), tabular to lenticular bodies, and are loose to moderately well-consolidated, weakly to moderately clay-cemented, weakly to strongly calcareous, and weakly to well-imbricated. Cross-stratification occurs in 1–20% of any given gravel body and includes trough to low-angle planar cross-bedding (foresets up to 1 m tall). Occasional lateral accretion sets and reverse grading. Gravel consist of mostly clast-supported (minor matrix-supported), very poorly to moderately sorted, subangular to rounded (mostly subrounded) pebbles (50–95%), cobbles (5–50%), and boulders (trace to 12%). Clast lithologies include fine-grained felsic volcanics, with 5–25% feldspar porphyries, 1–20% moderately crystal-rich felsites (>3% visible phenocrysts), and 0–15% intermediate volcanic clasts. Intermediate volcanics are <1% north of Crawford Hollow and crystal-rich felsites are mostly limited to proximal-medial deposits of the Nogal Canyon paleofan. Gravel matrix consists of subangular to rounded, very poorly to moderately sorted, mostly medium- to coarse-grained sand (<10–20% finer and 10–25% very coarse sand to granules) composed of 70–95% lithics (felsic volcanic) and 5–30% quartz + feldspar. Clay as pore linings or bridges is estimated to compose 0.5–15% of the matrix. It imparts an array of reddish colors, including light reddish-brown to reddish-brown or yellowish-red to reddish-yellow (5YR 5-6/3-4 or 4-6/6; 7.5YR 6/6). Locally, gravel matrix may be light-gray, light-brown, or strong brown (5-7.5YR 7/1; 7.5YR 6/4, 5/6). Fine-grained sediment is well-consolidated and occurs in thin to thick, tabular beds locally demarcated by clay-enriched zones at the top of a bed (probable paleosols). This sediment consists of a mixture of clay, silt, and very fine to fine sand with 1–30% scattered medium to very coarse sand grains and 1–10% pebbles. Beds are internally massive due to bioturbation and pedogenesis. Clay-rich zones are reddish-brown (5YR) and have angular to subangular blocky peds that are commonly coated by distinct illuviated clay films. Colors for fine-grained intervals include light-reddish-brown to pink (5YR 6/4; 7.5YR 7/3), but muddy beds locally range from light-yellowish-brown (2.5Y 6/3) to brown or pink (7.5YR 5/3 or 7/4). Buried stage I to II+ calcic horizons are locally present but minor in comparison to illuviated clay (Bt, Btk) horizons. To the south, strong calcium carbonate development is common in the upper 0.6–1.5 m of the unit, including stage III-III+ soil horizons, but buried soils are rare. Thickness is 50–85 m.

QTppm Middle Piedmont Facies of the Palomas Formation (Lower Pleistocene to Upper Pliocene) – Silty to sandy mud and silt in massive to laminated or very thin to thin, mostly tabular beds; subordinate silty sand or pebbly gravel in thin to thick (<40 cm), tabular to lenticular beds. Non- to weakly calcareous. Muddy beds are moderately to well-consolidated and mostly internally massive whereas sandy to gravelly beds are loose to moderately consolidated and may be internally massive to horizontal-planar laminated. Locally, unit consists of up to 80% mud with the remainder being a mix of silt, sand, and gravel. Mud is reddish-brown to light-reddish-brown, light-brown, or pink to very pale-brown (5YR 5-6/4; 7.5YR 7/3-4, 6/3-4;

10YR 7/3-4), often silty, and may contain trace to 5% subangular to rounded sand grains comprised of >80% lithics (volcanic). Rare to occasional buried calcic horizons (stage I-III) are up to 60 cm thick and characterized by carbonate nodules, tubules, or masses; these are sometimes associated with illuviated clay horizons (Bt or Btk). Rubbly weathering carbonate with possible root casts between Silver Canyon and Crawford Hollow near the top of the unit may represent *ciénega* (marsh) deposits. Sandy beds commonly consist of light-yellowish-brown or brown (10YR), well-sorted, subrounded to rounded, silty, vfU-fU grains composed of 65–70% quartz, 20–25% feldspar, and 10–15% lithics (black ferromagnesian minerals and volcanics) with little or no clay. Rare pebble gravels may be imbricated and consist of 55–60% fine-grained rhyolites and tuffs with 35–40% coarser grained felsites (>3% visible phenocrysts) and <5% intermediate volcanic lithologies. Gravels are distinctly lenticular and have a sandy matrix similar to sand beds described above that also lack clay. Where overlying Qppu contains higher proportions of finer-grained beds, QTppm may be distinguished by tanner colors (mostly 7.5YR) and greater lenticularity in channel-fill gravels that are less extensive and contain less matrix clay. Total thickness unknown but at least 45–60 m.

QTpaf Axial-fluvial facies of the Palomas Formation, floodplain deposits (Lower Pleistocene) – Reddish to pale-colored, mostly massive muds with subordinate sand lenses similar to those described for unit QTpa. Found in Crawford Hollow along the eastern quadrangle boundary and laterally gradational with distal piedmont facies of unit QTppm. Thickness on quadrangle is 3–7.5 m.

QTpa Axial-fluvial Facies of the Palomas Formation (Lower Pleistocene to Lower Pliocene) – Sand, lesser mud, and rare to occasional pebble gravel in laminated to thick (up to 90 cm), mostly lenticular beds. Sand is loose, non-calcareous, and internally massive to horizontal-planar or ripple cross-laminated to trough or planar cross-stratified (foresets up to 30 cm thick). Sand is composed of light-brownish-gray (10YR 6/2), poorly to moderately well-sorted, subrounded to rounded, vfL-cL grains (mostly fU-cL) composed of 60–70% quartz, 15–20% feldspar, and 15–20% lithics (volcanic, black ferromagnesian minerals, chert, and possible trace granite) with no clay. Notable brownish red to golden flakes of mica are also found in matrix (trace to 2%). Mud rip-up clasts up to 25 cm across are locally found in basal parts of sandy beds, particularly where scoured into mud. Mud is pale to very-pale-brown (2.5Y-10YR 8/2 and 2.5Y 7/3) or yellowish-red (5YR 4-5/6), weakly to moderately consolidated, non-calcareous, and massive to horizontal-planar laminated. It may contain whitish gypsum crusts, blades, and masses, particularly in and near Nogal and Silver Canyons. Pebble gravels (with very rare cobbles) occur in medium to thick (<20–30+ cm), lenticular beds. These are clast-supported and imbricated; clasts are poorly to moderately sorted and subrounded to well-rounded. Clast lithologies include subequal proportions of granite, chert/jasperoid, intermediate and felsic volcanics, undivided tuffs, and slightly more quartzite (15–20%). Rare pebbles of Pedernal chert are also found. Pebbles of similar lithologies are frequently concentrated at the base of individual crossbeds in sandy intervals. Gravel matrix is similar to sand but may contain trace or a few percent clay chips or bridges that impart a slightly reddish color. Basal scour by gravelly beds forms up to 0.6 m of relief along contacts with underlying sediment. Buried soils do not occur in gravels or sand but illuviated clay (Bt) horizons are observed in muddy intervals in a few places and indicated by mottling and prismatic peds. Fragments of fossil vertebrates are occasionally found in muds and sand; a partial vertebra of the glyptodont *Glyptotherium texanum* recovered approximately 1 km north of Silver Canyon suggests that the uppermost axial-fluvial strata are younger than 2.7 Ma (D. Gillette and G. Morgan, pers. comm., 2019). At least 60 m thick.

QTppml Lower to Middle Piedmont Facies of the Palomas Formation, undivided (Lower Pleistocene to Lower Pliocene) – Westward-thinning package of silty or sandy to gravelly sediment mapped in Nogal Canyon that includes units QTppm and Tppl. Intervals correlating to QTppm have fewer muddy beds compared to elsewhere on the quadrangle. See detailed descriptions of each unit. Thickness is <1–60 m.

Tppl Lower Piedmont Facies of the Palomas Formation (Lower Pliocene) – Poorly exposed, weakly to well-consolidated pebble-cobble-boulder gravel/conglomerate. Gravel/conglomerate are grayish, occasionally calcite-cemented, and massive to vaguely imbricated. Clasts consist of very poorly to poorly sorted, subangular to rounded pebbles (40–80%), cobbles (20–40%), and boulders (10–30%). Clast lithologies include 40–50% Vicks Peak Tuff, 45–50% undivided felsites (mostly fine-grained), and 0–15% greenish gray hornblende-plagioclase-phyric andesite. Unit forms an onlapping unconformity on Vicks Peak Tuff in the southwest part of the quadrangle. Thickness is unknown but likely <35–45 m.

Tsml Lower and Middle Santa Fe Group, piedmont facies (Middle to Lower? Miocene) – Yellowish to reddish or reddish-brown beds of sandstone and mudstone with subordinate conglomerate exposed along Nogal Canyon. Thickness is >90 m.

TERTIARY

Volcanic Rocks

Tvu Volcanic Rocks, undivided (Oligocene to Eocene?) – Undivided volcanic rocks exposed along Nogal Canyon. Probably Tuff of Rocque Ramos Canyon or trachyandesite in most places. See the following descriptions for the individual volcanic units.

Tvp Vicks Peak Tuff (Lower Oligocene) – Gray to light-gray (N6/ to N7/), weathering gray to reddish-brown, welded, crystal-poor, rhyolitic ash-flow tuff. Phenocrysts include trace to 3% sanidine (fine to coarse, subhedral to euhedral, glassy to chatoyant), trace to 1% mafics (fine, equant), and trace quartz. Trace lithics up to 1.5 cm long are aphanitic or contain some feldspar casts. Matrix is mostly devitrified but contains trace medium glass shards (dark/opaque). Occasional eutaxitic foliation, trace to minor (15%) fiamme, and sparse to abundant spherulites. A dark-gray to black vitrophyre is observed at the base of the Vicks Peak in the southern part of the map area. This vitrophyre contains similar sanidine phenocrysts and lithic fragments as the material above it but altered to clays. The unit forms steep slopes, ledges, or cliffs. $^{40}Ar/^{39}Ar$ age of 28.72 ± 0.02 Ma (sample 18BH-726). Thickness is <180 m.

Tvs Volcaniclastic Sediment Below Vicks Peak Tuff (Lower Oligocene) – Poorly exposed volcaniclastic sediment underlying Vicks Peak Tuff. Thickness is <6 m.

Tlj La Jencia Tuff (Lower Oligocene) – Purplish-brown or gray, weathering dark-purplish to very dark-brown, moderately to strongly welded, rhyolitic ash-flow tuff. Phenocrysts include 2–7% sanidine (fine to medium, subhedral to euhedral, glassy to chatoyant or altered to clay) and trace to 1% biotite (fine, subhedral, occasional coppery luster or altered to reddish, earthy mineral). Trace to 1% dusky to purplish-brown lithics up to 0.3 cm across are aphanitic or may contain tabular minerals altered to clay. Common eutaxitic foliation. Abundant fiamme and stretched vesicles and lapilli. Length:width ratios of fiamme highly variable, ranging from 3:1 to 76:1. Forms a thin ledge underlying the Vicks Peak Tuff east of New Mexico Highway 1, where it is inferred to have filled a paleotopographic low formed on the Tuff of Rocque Ramos Canyon. $^{40}Ar/^{39}Ar$ age of 29.00 ± 0.02 Ma (sample 18BH-724). Thickness is <7 m thick.

Trr Tuff of Rocque Ramos Canyon (Upper Eocene) – Light-gray to white (N8/; 2.5-5YR 8/1) or pinkish-gray to reddish-brown (5YR 8/1-6/2 to 4/3-4), weathering dark reddish-brown to dark-gray, moderately to densely welded ash-flow tuff. Compaction foliation is observed in places but is much more poorly developed than in the La Jencia Tuff. Phenocrysts occupy 15–40% of the surface area and are composed mainly of sanidine (fine to medium, subhedral to euhedral, glassy) with subordinate plagioclase (fine to medium, mostly subhedral) and trace to 7% biotite (fine, subhedral, commonly altered with coppery luster). The unit contains 1–5% pumice that are 1–10 cm long and relatively undeformed to highly flattened. At Black Hill, <10–15% pebble-sized lithic andesite fragments are present. South of Nogal Canyon, unit includes a reddish-brown to brown, ledge-forming, volcaniclastic facies underlying welded, sanidine-rich tuff. These facies have a mostly matrix-supported texture with subangular to subrounded, pebble-sized pumice and minor aphanitic andesite clasts. $^{40}Ar/^{39}Ar$ ages of 35.72 ± 0.01 Ma and 35.75 ± 0.01 Ma (samples 18BH-5DK and 18BH-749, respectively). Thickness is <80–100 m.

Tta Trachyandesite (Upper Eocene) – Purplish brown, weathering dark reddish or grayish brown, slightly to moderately vesicular, massive to moderately flow-foliated, aphanitic, trachyandesite lava. Vesicles are commonly coated by whitish to buff calcium carbonate or occasionally by ferromagnesian minerals. Phenocrysts include <2–3% total plagioclase, pyroxene, hornblende, and olivine; plagioclase and pyroxene are more common. Phenocrysts are very fine- to fine-grained (rare medium). Forms slopes and ledges. Exposed thickness is 65–70 m.

PALEOZOIC

IPu Pennsylvanian Rocks, undivided (Middle to Lower Pennsylvanian) – Medium to dark gray, mostly medium-bedded, non- to occasionally cherty, generally fossiliferous mudstone, wackestone, and packstone. Chert occurs as whitish lace that weathers orange-tan. Fossils include nautiloids, bivalves up to 1.25 cm in diameter, crinoids, sponge spicules, and fusulinids. The latter are up to 3.5 mm long and often lack internal structure due to recrystallization. Some mudstones are highly bioturbated with burrows up to 0.8 cm in diameter and occurring along bedding planes. Covered intervals are inferred to be underlain by shale. The thickness of the Pennsylvanian section at Bell Hill in the adjacent Steel Hill quadrangle (sections 17 and 20, T8S, R4W) is >495 m of which the Gray Mesa and Bar B Formations comprise 460–470 m (Lucas et al., 2017).

APPENDIX B

$^{40}Ar/^{39}Ar$ dating analyses from samples collected on the
Black Hill 7.5-minute quadrangle

Samples 18BH-724, 18BH-726, and 18BH-749 were collected from the La Jencia Tuff (Tlj), Vicks Peak Tuff (Tvp), and Tuff of Rocque Ramos Canyon (Trr), respectively. Sample 18BH-5DK was also collected from the Tuff of Rocque Ramos Canyon. The table below provides location data for each sample:

Sample	Unit	Age	Location*
18BH-749	Trr	35.75 ± 0.01 Ma	297263 mE, 3717281 mN
18BH-5DK	Trr	35.72 ± 0.01 Ma	295060 mE, 3718670 mN
18BH-724	Tlj	29.00 ± 0.02 Ma	293841 mE, 3709946 mN
18BH-726	Tvp	28.72 ± 0.02 Ma	293845 mE, 3709934 mN

* Location coordinates are given in NAD83 UTM Zone 13S.

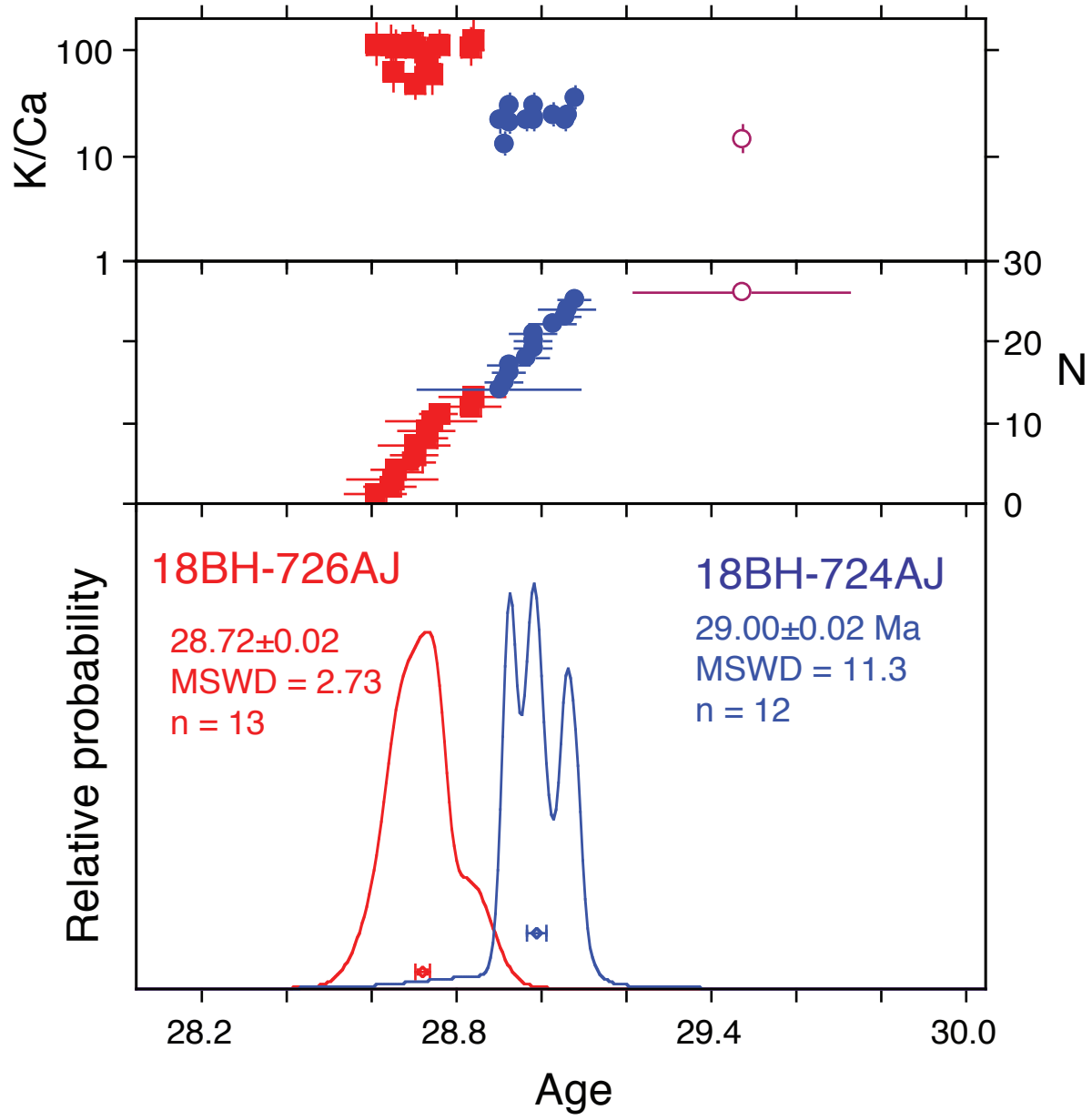
K/Ca
100
10
1
30
20
10
0
N
Relative probability
18BH-726AJ
28.72±0.02
MSWD = 2.73
n = 13
18BH-724AJ
29.00±0.02 Ma
MSWD = 11.3
n = 12
28.2
28.8
29.4
30.0
Age

Age-Probability Spectra for Samples 17PT-193, 18BH-5DK, and 18BH-749AJ

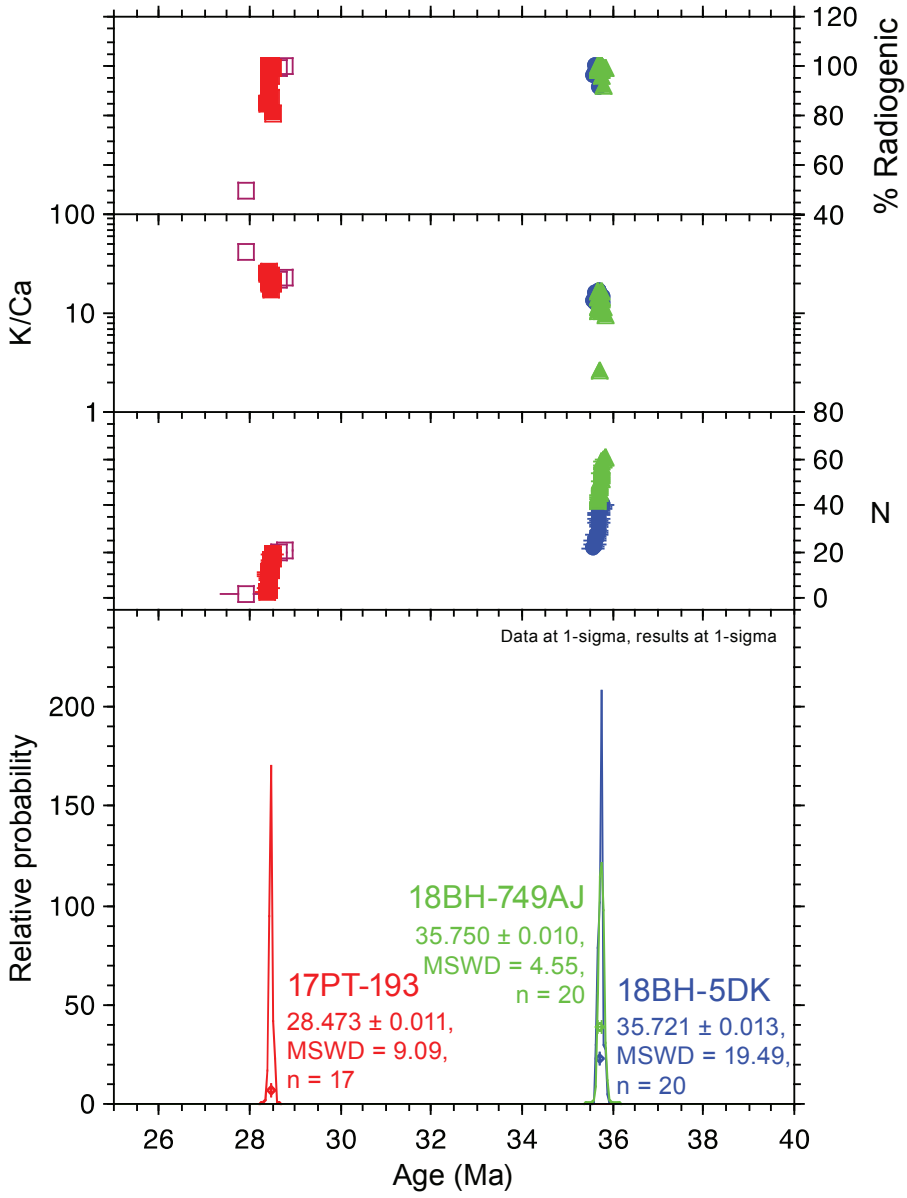

Red sample on Priest Tank 7.5-minute quadrangle

APPENDIX C

Clast count data from the Black Hill 7.5-minute quadrangle

This appendix contains tabulated clast count data (lithology type) from select geologic units exposed in the Black Hill quadrangle, including modern alluvium and Palomas Formation units. Clast counts were conducted by random selection of clasts of ≥0.5 cm diameter from 50-200 cm^2 areas of unit outcrops. The intermediate diameter of each clast was measured. Clast lithology categories are modified from Table 2 of Koning et al. (2016). Lithology abbreviations include: Psa = Permian San Andres Formation and Pay = Permian Abo and Yeso Formations, undivided. "San Mateo marker clast" refers to a distinct, sanidine-rich felsic volcanic lithology with shattered feldspar phenocrysts up to 1 cm across. The source area for this lithology is the southern San Mateo Mountains. Location coordinates for all counts are given in NAD83 UTM zone 13S.

TABLE C.1 CLAST-COUNT DATA FOR UNIT Qam (WAY-POINT 190328_6)

Date	03/28/19	*n = 105*
UTM Location	3713417N, 295403E	
	n	% total
Total felsic volcanics	38	36%
Crystal-poor felsic volcanics	23	22%
Crystal-rich felsic volcanics	15	14%
Tuffs, undivided	6	6%
“San Mateo” marker clast	6	6%
Vicks Peak Tuff	39	37%
Total intermediate volcanics	1	1%
Crystal-poor intermediate volcanics	0	0%
Crystal-rich intermediate volcanics	1	1%
Feldspar porphyry	0	0%
Paleozoic carbonates	8	8%
Psa + Pay	0	0%
Sandstone+siltstone, undivided	0	0%
Chert and jasperoid	0	0%
Granite	0	0%
Quartzite	0	0%
Vein quartz	0	0%
Basalt	0	0%
Other	7	7%
Comments	Crystal-poor felsite is mostly flow-banded rhyolite. Other = 3% unknown, 2% breccia, 1% volcaniclastic sandstone, and 1% vitrophyre.	

TABLE C.2 CLAST-COUNT DATA FOR UNIT Qppu (WAY-POINT 180912_1-3)

Date	09/12/18	*n = 99*
UTM Location	3710048N, 297525E	
	n	% total
Total felsic volcanics	30	30%
Crystal-poor felsic volcanics	17	17%
Crystal-rich felsic volcanics	13	13%
Tuffs, undivided	10	10%
“San Mateo” marker clast	22	22%
Vicks Peak Tuff	29	29%
Total intermediate volcanics	1	1%
Crystal-poor intermediate volcanics	0	0%
Crystal-rich intermediate volcanics	1	1%
Feldspar porphyry	3	3%
Paleozoic carbonates	0	0%
Psa + Pay	0	0%
Sandstone+siltstone, undivided	1	1%
Chert and jasperoid	0	0%
Basalt	0	0%
Other	3	3%
Comments	Tuffs, undivided includes 2% clasts of La Jencia tuff; Other = 3% unknown.	

TABLE C.3 CLAST-COUNT DATA FOR UNIT Qppu (WAY-POINT 180912_1-3b)

Date	09/12/18	*n = 59*
UTM Location	3710649N, 297595E	
	n	% total
Total felsic volcanics	21	21%
Crystal-poor felsic volcanics	10	10%
Crystal-rich felsic volcanics	11	11%
Tuffs, undivided	7	7%
“San Mateo” marker clast	3	3%
Vicks Peak Tuff	25	25%
Total intermediate volcanics	0	0%
Crystal-poor intermediate volcanics	0	0%
Crystal-rich intermediate volcanics	0	0%
Feldspar porphyry	0	0%
Paleozoic carbonates	0	0%
Psa + Pay	0	0%
Sandstone+siltstone, undivided	0	0%
Chert and jasperoid	0	0%
Basalt	0	0%
Other	3	3%
Comments	Other = 5% unknown.	

TABLE C.4 CLAST-COUNT DATA FOR UNIT Qppu (WAY-POINT 190213_2-3a)

Date	02/13/19	*n = 106*
UTM Location	3714135N, 301506E	
	n	% total
Total felsic volcanics	0	0%
Crystal-poor felsic volcanics	36	34%
Crystal-rich felsic volcanics	18	17%
Tuffs, undivided	23	22%
“San Mateo” marker clast	3	3%
Vicks Peak Tuff	21	20%
Total intermediate volcanics	0	0%
Crystal-poor intermediate volcanics	0	0%
Crystal-rich intermediate volcanics	1	1%
Feldspar porphyry	0	0%
Paleozoic carbonates	0	0%
Psa + Pay	0	0%
Sandstone+siltstone, undivided	0	0%
Chert and jasperoid	0	0%
Basalt	0	0%
Other	4	4%
Comments	Tuffs, undivided includes 3% clasts of La Jencia tuff; other = 1% pumice, 1% breccia, and 2% unknown.	

TABLE C.5 CLAST-COUNT DATA FOR UNIT QTppm (WAY-POINT 190221_2-1e)		
Date	02/21/19	*n = 98*
UTM Location	3717577N, 302564E	
	n	% total
Total felsic volcanics	38	39%
Crystal-poor felsic volcanics	17	17%
Crystal-rich felsic volcanics	21	21%
Tuffs, undivided	23	23%
“San Mateo” marker clast	6	6%
Vicks Peak Tuff	26	27%
Total intermediate volcanics	2	2%
Crystal-poor intermediate volcanics	1	1%
Crystal-rich intermediate volcanics	1	1%
Feldspar porphyry	0	0%
Paleozoic carbonates	0	0%
Psa + Pay	0	0%
Sandstone+siltstone, undivided	0	0%
Chert and jasperoid	0	0%
Basalt	0	0%
Other	3	3%
Comments	Other = 2% unknown, 1% silicic intrusive.	

TABLE C.6 CLAST-COUNT DATA FOR UNIT QTpa (WAY-POINT 180913_2-1i)		
Date	09/13/18	*n = 100*
UTM Location	3710438N, 302038E	
	n	% total
Total felsic volcanics	12	12%
Crystal-poor felsic volcanics	8	8%
Crystal-rich felsic volcanics	4	4%
Tuffs, undivided	14	14%
“San Mateo” marker clast	0	0%
Vicks Peak Tuff	4	4%
Total intermediate volcanics	14	14%
Crystal-poor intermediate volcanics	3	3%
Crystal-rich intermediate volcanics	11	11%
Feldspar porphyry	0	0%
Paleozoic carbonates	2	2%
Psa + Pay	2	2%
Sandstone+siltstone, undivided	2	2%
Chert and jasperoid	13	13%
Granite	14	14%
Quartzite	18	18%
Vein quartz	4	4%
Basalt	0	0%
Other	1	1%
Comments	Chert and jasperoid includes 4% clasts of Pedernal chert; Other = 1% unknown.	

TABLE C.7 CLAST-COUNT DATA FOR UNIT Tppl (WAY-POINT 190328_1c)		
Date	03/28/19	*n = 98*
UTM Location	3710696N, 291654E	
	n	% total
Total felsic volcanics	44	45%
Crystal-poor felsic volcanics	30	31%
Crystal-rich felsic volcanics	14	14%
Tuffs, undivided	4	4%
“San Mateo” marker clast	0	0%
Vicks Peak Tuff	39	40%
Total intermediate volcanics	6	6%
Crystal-poor intermediate volcanics	6	6%
Crystal-rich intermediate volcanics	0	0%
Feldspar porphyry	0	0%
Paleozoic carbonates	0	0%
Psa + Pay	0	0%
Sandstone+siltstone, undivided	0	0%
Chert and jasperoid	0	0%
Granite	0	0%
Quartzite	0	0%
Vein quartz	0	0%
Basalt	0	0%
Other	5	5%
Comments	Crystal-poor felsite is mostly flow-banded rhyolite. Other = 2% intrusive (dioritic?), 2% unknown, and 1% volcaniclastic.	

APPENDIX D

Maximum clast size data from the Black Hill 7.5-minute quadrangle

Maximum clast size measurements were made of the 10 largest clasts in an area of approximately 75-100 m^2. The longest (a) and intermediate (b) axes of each clast were measured. Clast lithologies were noted as well; lithology abbreviations include: Tvp = Vicks Peak Tuff and Trr = Tuff of Rocque Ramos Canyon. All UTM coordinates are given in NAD83 UTM zone 13S.

TABLE D.1 MAXIMUM CLAST SIZE MEASUREMENTS AT WAYPOINT 190212_1-4d

Silver Canyon		a axis (cm)	b axis (cm)	Lithology
Northing	3711886	40.5	25	Tvp
Easting	302400	58	30.5	Crystal-rich felsite
Unit	Qam	32.5	26.5	Undivided tuff
Mean (a axis)	40	41	25	Tvp
Median (a axis)	39	37.5	23	Crystal-rich felsite
Mean (b axis)	25	42.5	29	Undivided tuff
Median (b axis)	25	36	22	Crystal-rich felsite
n	10	35.5	22	Tvp
		42	25.5	Undivided tuff
		32	21	Crystal-poor felsite

TABLE D.2 MAXIMUM CLAST SIZE MEASUREMENTS AT WAYPOINT 190328_6

Nogal Canyon		a axis (cm)	b axis (cm)	Lithology
Northing	3713417	49.5	46	Tvp
Easting	295403	49.5	25.5	Crystal-rich felsite
Unit	Qam	46	19	Crystal-rich felsite
Mean (a axis)	44	51	35.5	Crystal-rich felsite
Median (a axis)	45	53	29.5	Tvp
Mean (b axis)	31	42	37	Undivided tuff
Median (b axis)	29.5	38	29.5	Tvp
n	10	33.5	31	Vitrophyre
		34	27.5	Crystal-rich felsite
		43.5	29.5	Crystal-rich felsite

TABLE D.3 MAXIMUM CLAST SIZE MEASUREMENTS AT WAYPOINT 180912_1-3

		a axis (cm)	b axis (cm)	Lithology
Northing	3710048	33.5	22	Tvp
Easting	297525	26	15.5	Crystal-poor felsite
Unit	Qppu	29	23	Crystal-rich felsite
Mean (a axis)	27	26	18	Tvp
Median (a axis)	26	26.5	19	Tvp
Mean (b axis)	17	20	20	Tvp
Median (b axis)	16.75	25.5	14.5	Tvp
n	10	25	15	Crystal-poor felsite
		24.5	11	Tvp
		33	15	Undivided tuff

TABLE D.4 MAXIMUM CLAST SIZE MEASUREMENTS AT WAYPOINT 190212-2				
		a axis (cm)	b axis (cm)	Lithology
Northing	3715689	23	18	Crystal-poor felsite
Easting	300537	23.5	19.5	Tvp
Unit	Qppu	25.5	12.5	Crystal-poor felsite
Mean (a axis)	22	24	14.5	Crystal-poor felsite
Median (a axis)	21	18.5	11	Crystal-poor felsite
Mean (b axis)	14	20.5	13	Crystal-poor felsite
Median (b axis)	13	20	9	Crystal-rich felsite
n	10	19	13	Feldspar porphyry
		19.5	14.5	Crystal-poor felsite
		21.5	12	Crystal-rich felsite

TABLE D.5 MAXIMUM CLAST SIZE MEASUREMENTS AT WAYPOINT 190212-2				
		a axis (cm)	b axis (cm)	Lithology
Northing	3712466	26.5	9	Crystal-rich felsite
Easting	301418	15	13.5	Crystal-rich felsite
Unit	Qppu	26	14	Undivided tuff
Mean (a axis)	19	14	12	Undivided tuff
Median (a axis)	17	15	12	Undivided tuff
Mean (b axis)	12	17	11	Crystal-poor felsite
Median (b axis)	12	17.5	13.5	Crystal-poor felsite
n	10	15.5	11.5	Crystal-rich felsite
		16	14	Tvp
		22.5	11.5	Tvp

TABLE D.6 MAXIMUM CLAST SIZE MEASUREMENTS AT WAYPOINT 190221_2-1e				
		a axis (cm)	b axis (cm)	Lithology
Northing	3717577	12	5.5	Crystal-poor felsite
Easting	302564	12	7	Tvp
Unit	QTppm	11	7	Tvp
Mean (a axis)	11	10	6	Trr?
Median (a axis)	11	9.5	6.5	Crystal-rich felsite
Mean (b axis)	7	10	6.5	Tvp
Median (b axis)	7	8.5	8	Tvp
n	10	13.5	8	Crystal-rich felsite
		10.5	7	Crystal-rich felsite
		11	7.5	Crystal-poor felsite

TABLE D.7 MAXIMUM CLAST SIZE MEASUREMENTS AT WAYPOINT 190328_1c				
		a axis (cm)	b axis (cm)	Lithology
Northing	3710696	45	44.5	Tvp
Easting	291654	61	50.5	Tvp
Unit	Tppl	62.5	36	Crystal-rich felsite
Mean (a axis)	60	53	35	Crystal-rich felsite
Median (a axis)	60	54	37	Crystal-rich felsite
Mean (b axis)	40	65.5	48	Crystal-rich felsite
Median (b axis)	40.5	73	44	Tvp
n	10	58.5	36	Crystal-rich felsite
		58	26.5	Tvp
		66	44.5	Crystal-poor felsite

APPENDIX E

Paleocurrent data from the Black Hill 7.5-minute quadrangle

This appendix contains tabulated paleocurrent direction data (azimuthal) measured from imbrication of gravels and channel axes and margins from Palomas Formation units exposed in the Black Hill quadrangle. A Brunton pocket transit was used for all measurements. Location coordinates for all measurements are given in NAD83 UTM zone 13S. Mean paleocurrent directions are shown on the geologic map.

TABLE E.1 IMBRICATION PALEOCURRENT MEASUREMENTS AT WAYPOINT 180516_3										
		Flow direction measurements								
Northing	3712451	120	120	139	128	137	145			
Easting	296015	120	120	131	128	133	127			
Unit	Qppu	120	139	131	166	133	127			
Mean	132	120	139	131	166	135	127			
Median	134	120	139	149	135	135	134			
n	57	120	139	149	135	135	139			
		120	139	100	135	145	139			
		120	139	100	125	145				
		120	139	128	125	145				
		120	139	128	137	145				

TABLE E.2 IMBRICATION PALEOCURRENT MEASUREMENTS AT WAYPOINT 180912_1-1b										
		Flow direction measurements								
Northing	3709190	146	154	191	181					
Easting	298433	146	160	156	181					
Unit	Qppu	163	160	156	155					
Mean	168	163	160	194	155					
Median	163	163	160	194	141					
n	35	163	160	175						
		163	191	175						
		154	191	175						
		154	191	175						
		154	191	181						

TABLE E.3 IMBRICATION PALEOCURRENT MEASUREMENTS AT WAYPOINT 180912_1-2e										
		Flow direction measurements								
Northing	3709851	92	150	112	92	107				
Easting	299100	92	150	112	92	161				
Unit	Qppu	66	96	112	96	161				
Mean	108	66	96	112	96					
Median	96	66	96	112	115					
n	43	66	96	92	115					
		150	96	92	115					
		150	96	92	107					
		150	96	92	107					
		150	112	92	107					

TABLE E.4 IMBRICATION PALEOCURRENT MEASUREMENTS AT WAYPOINT 180912_1-3										
		Flow direction measurements								
Northing	3710048	93	89	170	145	148	104			
Easting	297525	93	89	170	145	88	104			
Unit	Qppu	93	142	154	121	88	141			
Mean	130	167	142	154	98	100	141			
Median	141	167	161	154	98	100	141			
n	56	167	129	154	109	100	141			
		160	129	154	109	147				
		160	129	145	109	147				
		89	170	145	109	147				
		89	170	145	148	104				

TABLE E.5 IMBRICATION PALEOCURRENT MEASUREMENTS AT WAYPOINT 180912A_1-3e										
		Flow direction measurements								
Northing	3710975	153	120	80						
Easting	297141	153	120	80						
Unit	Qppu	153	120	100						
Mean	114	153	120	100						
Median	110	153	110	100						
n	29	153	110	81						
		153	80	81						
		125	80	109						
		125	80	109						
		125	80							

TABLE E.6 IMBRICATION PALEOCURRENT MEASUREMENTS AT WAYPOINT 180912B_1-3e										
		Flow direction measurements								
Northing	3710975	160	157	88						
Easting	297141	160	157	119						
Unit	Qppu	160	157	119						
Mean	125	121	91	79						
Median	125	121	91	79						
n	27	125	138	79						
		125	138	79						
		157	138							
		157	138							
		157	88							

TABLE E.7 IMBRICATION PALEOCURRENT MEASUREMENTS AT WAYPOINT 181108_2e										
		Flow direction measurements								
Northing	3711866	69	96	123	95					
Easting	300974	69	125	96	97					
Unit	Qppu	69	125	96	97					
Mean	89	69	87	91						
Median	91	69	87	91						
n	33	54	87	91						
		54	85	105						
		56	85	95						
		104	85	95						
		96	85	95						

TABLE E.8 IMBRICATION PALEOCURRENT MEASUREMENTS AT WAYPOINT 181108_3b										
		Flow direction measurements								
Northing	3712340	123	133	107	102					
Easting	300636	123	133	152	102					
Unit	Qppu	123	133	152	102					
Mean	124	133	133	119	102					
Median	130	133	122	119	102					
n	37	133	122	128	99					
		133	122	128	99					
		133	135	130						
		133	135	130						
		133	135	130						

TABLE E.9 IMBRICATION PALEOCURRENT MEASUREMENTS AT WAYPOINT 190212_1-3c										
		Flow direction measurements								
Northing	3713021	140	165	110	161					
Easting	300655	140	165	180	154					
Unit	Qppu	140	107	180	154					
Mean	137	144	107	112	154					
Median	140	144	155	112	154					
n	35	120	126	112						
		114	126	112						
		165	126	110						
		165	126	110						
		165	90	161						

TABLE E.10 IMBRICATION PALEOCURRENT MEASUREMENTS AT WAYPOINT 190212_1-3h										
		Flow direction measurements								
Northing	3713096	176	174	131	165					
Easting	301205	147	113	131	158					
Unit	Qppu	147	113	131	158					
Mean	152	147	150	131	166					
Median	156	147	150	107	167					
n	37	174	150	107	167					
		174	156	170	167					
		174	156	170						
		174	159	140						
		174	159	140						

TABLE E.11 IMBRICATION PALEOCURRENT MEASUREMENTS AT WAYPOINT 190213_2-2b										
		Flow direction measurements								
Northing	3714169	106	93	78	89	86	135			
Easting	302180	106	93	78	91	86				
Unit	Qppu	144	95	78	139	86				
Mean	115	144	95	129	139	158				
Median	115	144	137	129	139	158				
n	51	145	137	115	139	104				
		145	137	115	105	104				
		145	137	115	105	135				
		93	78	115	105	135				
		93	78	89	105	135				

TABLE E.12 IMBRICATION PALEOCURRENT MEASUREMENTS AT WAYPOINT 190213_2-4a										
		Flow direction measurements								
Northing	3714820	146	147	194	141	177				
Easting	301855	146	147	194	141	177				
Unit	Qppu	146	184	194	141	171				
Mean	162	146	184	158	141	171				
Median	158	146	184	158	139	165				
n	50	143	170	197	139	165				
		143	146	197	139	165				
		143	146	197	177	165				
		143	146	172	177	146				
		143	194	172	177	146				

TABLE E.13 IMBRICATION PALEOCURRENT MEASUREMENTS AT WAYPOINT 190213_2-6a										
		Flow direction measurements								
Northing	3715138	140	93	89	100	157				
Easting	302401	140	93	89	100	157				
Unit	Qppu	140	111	105	152	125				
Mean	113	105	111	105	152	125				
Median	105	105	111	105	95	114				
n	45	105	111	125	95					
		141	105	125	95					
		93	105	125	99					
		93	105	100	99					
		93	105	100	157					

TABLE E.14 IMBRICATION PALEOCURRENT MEASUREMENTS AT WAYPOINT 190214_3-1a										
		Flow direction measurements								
Northing	3712724	111	152	160	113	160	166			
Easting	297706	111	152	160	113	160	166			
Unit	Qppu	111	152	149	106	160	166			
Mean	131	111	152	149	106	85	108			
Median	115	111	152	115	106	85	108			
n	57	111	114	115	106	85	108			
		146	114	115	106	85	108			
		146	114	115	179	161				
		146	114	115	179	161				
		146	160	113	160	161				

TABLE E.15 IMBRICATION PALEOCURRENT MEASUREMENTS AT WAYPOINT 190214_3-1c										
		Flow direction measurements								
Northing	3712376	50	114	104	102	132	96			
Easting	298069	50	114	104	70	132	96			
Unit	Qppu	50	114	104	70	132				
Mean	100	92	114	80	112	115				
Median	100	92	101	80	112	115				
n	52	92	101	94	112	115				
		83	101	94	112	142				
		83	98	94	130	142				
		83	98	94	100	96				
		83	98	102	100	96				

TABLE E.16 IMBRICATION PALEOCURRENT MEASUREMENTS AT WAYPOINT 190214_3-2										
		Flow direction measurements								
Northing	3712495	139	150	130	159	150				
Easting	297391	139	190	166	159	88				
Unit	Qppu	139	190	125	100	88				
Mean	131	139	190	125	100	88				
Median	125	105	190	125	100	88				
n	50	105	118	125	100	88				
		105	118	125	100	120				
		105	118	139	100	120				
		150	184	139	195	120				
		150	130	139	150	120				

TABLE E.17 IMBRICATION PALEOCURRENT MEASUREMENTS AT WAYPOINT 190220_1-1d										
		Flow direction measurements								
Northing	3716723	140	120	187						
Easting	302488	140	120	187						
Unit	Qppu	140	120	196						
Mean	144	140	159	196						
Median	140	140	159	95						
n	30	140	159	137						
		95	159	180						
		95	159	130						
		120	159	130						
		120	159	130						

TABLE E.18 IMBRICATION PALEOCURRENT MEASUREMENTS AT WAYPOINT 190220_1-2c										
		Flow direction measurements								
Northing	3716077	180	157							
Easting	302214	180	157							
Unit	Qppu	180	157							
Mean	165	180	168							
Median	168	143	168							
n	18	143	168							
		174	168							
		174	168							
		150								
		150								

TABLE E.19 IMBRICATION PALEOCURRENT MEASUREMENTS AT WAYPOINT 190220_1-2e										
		Flow direction measurements								
Northing	3716180	160	127	130	143	100				
Easting	301507	160	127	130	143	100				
Unit	Qppu	160	127	130	143	100				
Mean	133	160	148	130	130	101				
Median	130	160	148	161	130	101				
n	49	160	166	161	130	115				
		160	166	161	122	115				
		160	115	161	122	115				
		74	115	161	100	115				
		74	115	161	100					

TABLE E.20 IMBRICATION PALEOCURRENT MEASUREMENTS AT WAYPOINT 190319_1a										
		Flow direction measurements								
Northing	3714928	69	80	92	135	74	61	144		
Easting	300673	69	80	92	135	74	61	96		
Unit	Qppu	69	80	92	135	70	96	96		
Mean	83	69	80	95	59	70	96			
Median	74	116	60	95	59	70	73			
n	63	116	60	95	58	49	73			
		104	60	50	58	49	73			
		104	60	50	58	49	144			
		80	60	50	74	129	144			
		80	92	50	74	129	144			

TABLE E.21 CHANNEL MARGIN PALEOCURRENT MEASUREMENTS AT WAYPOINT 190319_1i										
		Flow direction measurements								
Northing	3715689	133								
Easting	300537	124								
Unit	Qppu	113								
Mean	123									
Median	124									
n	3									

TABLE E.22 IMBRICATION PALEOCURRENT MEASUREMENTS AT WAYPOINT 190319_2a										
		Flow direction measurements								
Northing	3716629	89	135	71	30	42	81	56		
Easting	300220	89	135	71	30	42	60	56		
Unit	Qppu	89	56	71	30	42	60	56		
Mean	78	89	56	74	30	42	100	96		
Median	74	89	56	74	30	42	100	96		
n	66	89	56	74	96	42	100	96		
		89	56	144	96	54	91			
		89	56	144	96	54	91			
		89	60	144	141	54	91			
		89	60	144	141	81	56			

TABLE E.23 IMBRICATION PALEOCURRENT MEASUREMENTS AT WAYPOINT 190319_2f										
		Flow direction measurements								
Northing	3717588	145	155	79	116	69				
Easting	300838	145	120	79	116	165				
Unit	Qppu	145	120	134	129	165				
Mean	118	107	120	134	129	114				
Median	120	107	120	134	83	114				
n	46	107	128	115	83	114				
		107	128	115	83					
		107	128	147	69					
		139	140	147	69					
		155	140	116	69					

TABLE E.24 IMBRICATION PALEOCURRENT MEASUREMENTS AT WAYPOINT 190328_1d										
		Flow direction measurements								
Northing	3710237	60	114	78						
Easting	293464	60	123	78						
Unit	Qppu	60	123	97						
Mean	88	60	123	97						
Median	96	60	123	97						
n	28	60	63	97						
		95	63	97						
		114	63	97						
		114	63							
		114	78							

TABLE E.25 IMBRICATION PALEOCURRENT MEASUREMENTS AT WAYPOINT 190328_3a										
		Flow direction measurements								
Northing	3712566	106	133	149	90	155				
Easting	296187	106	133	149	90	155				
Unit	Qppu	106	133	149	90	115				
Mean	134	106	133	170	154	115				
Median	136	106	133	170	154	124				
n	48	136	142	170	154	124				
		136	142	170	154	124				
		136	142	135	134	124				
		136	136	135	134					
		136	136	135	155					

TABLE E.26 IMBRICATION PALEOCURRENT MEASUREMENTS AT WAYPOINT 190328A_5										
		Flow direction measurements								
Northing	3713141	137	81	145						
Easting	296891	137	81	145						
Unit	Qppu	137	81	145						
Mean	133	137	81	147						
Median	145	154	142	147						
n	25	154	142							
		159	142							
		159	145							
		159	145							
		81	145							

TABLE E.27 IMBRICATION PALEOCURRENT MEASUREMENTS AT WAYPOINT 190328B_5										
		Flow direction measurements								
Northing	3713141	171	136	160	166					
Easting	296891	171	136	160	173					
Unit	Qppu	171	119	131	173					
Mean	157	168	119	131	173					
Median	163	168	155	156	183					
n	36	168	155	156	183					
		168	155	156						
		132	172	156						
		132	172	166						
		132	177	166						

TABLE E.28 IMBRICATION PALEOCURRENT MEASUREMENTS AT WAYPOINT 190404_1										
		Flow direction measurements								
Northing	3710761	155	21	165	145					
Easting	294340	155	21	165	145					
Unit	Qppu	155	204	165	198					
Mean	184	155	204	197	198					
Median	190	166	204	197	182					
n	38	166	214	197	177					
		205	214	197	177					
		205	214	197	177					
		205	214	206						
		21	165	206						

TABLE E.29 IMBRICATION PALEOCURRENT MEASUREMENTS AT WAYPOINT 180912_1-2b										
		Flow direction measurements								
Northing	3709626	117	124	114	106	159	106			
Easting	298866	117	124	114	106	125	106			
Unit	QTppm	117	124	150	106	125				
Mean	122	117	140	150	106	125				
Median	124	117	140	150	164	59				
n	52	117	140	135	164	103				
		136	140	135	164	103				
		136	140	135	74	103				
		136	140	135	74	103				
		124	114	106	74	106				

TABLE E.30 IMBRICATION PALEOCURRENT MEASUREMENTS AT WAYPOINT 181108_2										
		Flow direction measurements								
Northing	3711667	115	146	134	106	56	61	88		
Easting	300085	115	51	55	106	56	61	88		
Unit	QTppm	104	51	55	106	56	61			
Mean	95	104	93	73	132	88	76			
Median	88	104	95	73	132	88	76			
n	62	104	95	73	132	88	76			
		115	72	73	132	88	138			
		115	134	127	63	88	138			
		146	134	127	63	61	88			
		146	134	106	63	61	88			

TABLE E.31 IMBRICATION PALEOCURRENT MEASUREMENTS AT WAYPOINT 180913_2-1h										
		Flow direction measurements								
Northing	3710427	155	157	169	151	168	168			
Easting	302021	155	165	169	170	131	168			
Unit	QTpa	152	165	169	170	131				
Mean	164	152	165	169	170	176				
Median	168	152	165	169	170	176				
n	52	152	165	169	170	217				
		147	191	157	168	168				
		157	191	157	168	168				
		157	191	108	168	168				
		157	191	151	168	168				

TABLE E.32 CHANNEL AXES PALEOCURRENT MEASUREMENTS AT WAYPOINT 180913_2-2c										
		Flow direction measurements								
Northing	3709849	159								
Easting	302149	205								
Unit	QTpa	224								
Mean	196									
Median	205									
n	3									

TABLE E.33 IMBRICATION PALEOCURRENT MEASUREMENTS AT WAYPOINT 190328_1b										
		Flow direction measurements								
Northing	3710674	122	189	124	104	118				
Easting	291626	122	189	124	104					
Unit	Tppl	122	189	124	104					
Mean	120	122	153	95	104					
Median	122	122	153	95	125					
n	41	122	109	95	125					
		122	109	56	125					
		122	109	56	114					
		144	109	104	114					
		144	109	104	118					